

REPORT DOCUMENTATION PAGE

AFRL-SR-AR-TR-03-

02/16
ig the
using
02-
rrently

Public reporting burden for this collection of information is estimated to average 1 hour per response, including the time for reviewing data needed, and completing and reviewing this collection of information. Send comments regarding this burden estimate or any other burden to Department of Defense, Washington Headquarters Services, Directorate for Information Operations and Reports (070-4302). Respondents should be aware that notwithstanding any other provision of law, no person shall be subject to any penalty for failing to valid OMB control number. PLEASE DO NOT RETURN YOUR FORM TO THE ABOVE ADDRESS.

1. REPORT DATE (DD-MM-YYYY) 31-12-2002		2. REPORT TYPE Final Progress Report		3. DATES COVERED (From - To) 1 Nov 1999- 31 Oct 2002	
4. TITLE AND SUBTITLE Mechanisms of Photorefractivity in Polymeric Materials				5a. CONTRACT NUMBER	
				5b. GRANT NUMBER F49620-00-1-0038	
				5c. PROGRAM ELEMENT NUMBER	
6. AUTHOR(S) W. E. Moerner, R. J. Twieg				5d. PROJECT NUMBER 2303 /CV	
				5e. TASK NUMBER	
				5f. WORK UNIT NUMBER	
7. PERFORMING ORGANIZATION NAME(S) AND ADDRESS(ES) Stanford Leland Junior University 651 Serra Street, Room 260 Stanford, CA 94305-1525				8. PERFORMING ORGANIZATION REPORT NUMBER	
9. SPONSORING / MONITORING AGENCY NAME(S) AND ADDRESS(ES) AFOSR/NL Dr. Charles Y-C. Lee 801 N. Randolph St. Room 732 Arlington, VA 22203-1977				10. SPONSOR/MONITOR'S ACRONYM(S)	
				11. SPONSOR/MONITOR'S REPORT NUMBER(S)	
12. DISTRIBUTION / AVAILABILITY STATEMENT This document is approved for public release; its distribution is unlimited.					
13. SUPPLEMENTARY NOTES 20030220 048					
14. ABSTRACT This grant features a dual-edged effort of physical measurement (at Stanford) and synthesis (at the Kent State subcontractor) to develop new photorefractive polymers, demonstrate previously unobserved physical effects, and most importantly, to understand the mechanisms controlling the performance. This collaboration between Stanford and Kent, has successfully developed several new classes of materials which have been explored in detail using thermal, optical, electrical, and photorefractive measurements. Using our faster materials, we have demonstrated two new applications for photorefractive polymers: image amplification/novelty filtering, near-infrared response in a glassy photorefractive, and adaptive beamplitting for detection of laser-generated ultrasound.					
15. SUBJECT TERMS photorefractive polymers, optical processing, image amplification					
16. SECURITY CLASSIFICATION OF: a. REPORT unclassified			17. LIMITATION OF ABSTRACT none	18. NUMBER OF PAGES 37	19a. NAME OF RESPONSIBLE PERSON W. E. Moerner
b. ABSTRACT unclassified					19b. TELEPHONE NUMBER (include area code) 650-723-1727
c. THIS PAGE unclassified					

FINAL PROGRESS REPORT

MECHANISMS OF PHOTOREFRACTIVITY IN POLYMERIC MATERIALS

Principal Investigator: Prof. W. E. Moerner
Department of Chemistry, Stanford University
Mail Code 5080, 333 Campus Drive
Stanford, California 94305-5080
650-723-1727 (office), 650-725-0259 (fax), e-mail: moerner@stanford.edu

Subcontract Principal Investigator: Prof. Robert J. Twieg
Department of Chemistry, Kent State University
Kent, OH 44242
330-672-2791 (office), 330-672-3816 (fax), e-mail: rtwieg@lci.kent.edu

AFOSR Grant No. F49620-00-1-0038

Period Covered: 1 Nov 1999 - 31 Oct 2002

Date: 31 Dec 2002

2. Objectives:

The primary objective of this research effort has been to explore the detailed mechanisms responsible for the photorefractive effect in novel high-performance polymeric and liquid-crystalline materials with the aim of understanding speed, mobility, nonlinearity, and trap dynamics, thus uncovering critical structure-function relationships necessary for optimization for specific applications.

3. Status of Effort:

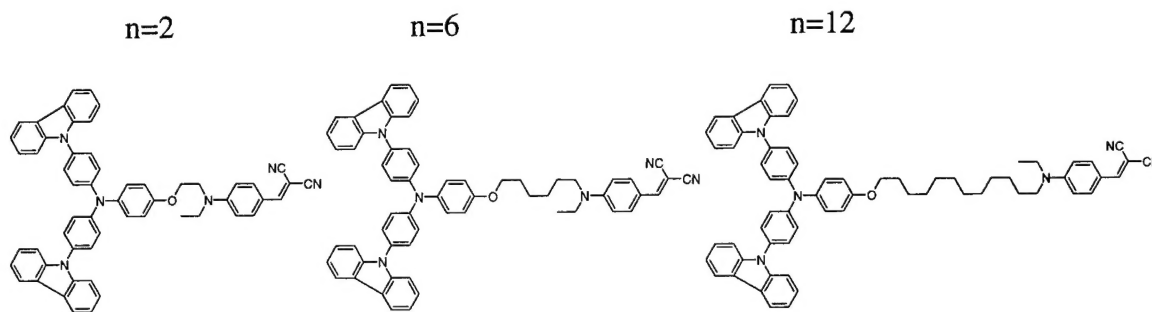
This grant has featured a dual-edged effort of physical measurement (at Stanford) and synthesis (at Kent State) to develop new photorefractive polymers and photorefractive glasses, demonstrate previously unobserved physical effects, and most importantly, to understand the mechanisms controlling the performance. Synthetic efforts have proceeded on several fronts, with the generation of new glassy monomeric materials, new plasticizers, and a new class of NLO chromophores. In the characterization efforts, a series of dual-function glassy monomers have been explored in which the charge transport agent is covalently linked to the NLO chromophore. A primary area of interest continues to be the speed of photorefractive response, as this is one of the few properties whose optimization would lead to new applications. Of course, higher speed without strong photorefractive response would not lead to a useful material, and vice versa. Using one of the newly designed NLO chromophores containing a novel dicyanodihydrofuran (DCDHF) acceptor, we have fabricated and developed composites that show both very high gain coefficients as well as high speed. Twenty-seven derivatives of this new chromophore have been synthesized and studied in a variety of physical, optical, and electric experiments. Many members of this new class form glasses when a monolithic sample is prepared, yielding strong beam fanning as well as large steady-state photorefractive response. These glasses have been explored in great detail as a function of ambient temperature, and one of the glasses shows excellent gain and good speed at 830 nm in the near infrared. Finally, to assist in the laser protection research program, we have interacted on multiple occasions with Mark Kuzyk to refine and simulate designs that utilize the photorefractive effect for optical limiting. We have also provided samples to Mark Kuzyk and Fassil Gebrehmichael.

4. Accomplishments/New Findings:

A. Synthetic Efforts – Glassy photorefractive monomers with covalent attachment of transport agent and NLO chromophore (NLO-DCTAs)

The idea of covalently binding the constituents of the PR mixture in a single multifunctional unit in order to avoid crystallization or phase separation of the components has been further studied. In prior work, the Bayreuth group investigated DR1-DCTA (4,4'-di(carbazol-9-yl)-4''-(2-[N-ethyl-N-[4-(nitrophenylazo)phenyl]amine]ethoxy) triphenylamine. Hohle, C.; Hofmann, U.; Schloter, S.; Thelakkat, M.; Strohriegl, P.; Haarer, D.; Zilker, S. *J. Mater. Chem.* 1999, 9, 2205). This molecule has a DR1 type chromophore and a triarylamine moiety as hole transporting medium. Unfortunately, the highly photochromic $-N=N-$ bond in the DR1 moiety produces large non-photorefractive gratings if the operating laser wavelength is only slightly in the absorption band of the chromophore. To avoid the undesired

photochromic grating, we have synthesized new NLO-DCTA molecules utilizing DCST (an aminodicyanostyrene) as the birefringent and nonlinear chromophore. Furthermore, DR1-DCTA has a linker between the charge transport and the chromophore with only two carbons. The length of the linking unit influences the glass transition temperature of the system which in turn influences the speed of chromophore orientation and photorefractive performance. Glasses with different linking lengths (DCTA-nC-DCST, $n = 2, 6$ and 12 carbons) between the charge transport and the chromophore have been made in our study.



	T _g	E _{OX1} [V]	HOMO [eV]
DCTA-2C-DCST	113 °C	0.83	-5.19
DCTA-6C-DCST	87 °C	0.82	-5.18
DCTA-12C-DCST	67 °C	0.82	-5.18

B. Synthetic Efforts: Plasticizers

In our prior research, we have shown that all the components in the photorefractive composite affect the charge transport, especially the trapping dynamics (A. Grunnet-Jepsen, D. Wright, B. Smith, M. S. Bratcher, M. S. DeClue, J. S. Siegel, and W. E. Moerner, "Spectroscopic Determination of Trap Density in C₆₀-Sensitized Photorefractive Polymers," *Chem. Phys. Lett.* **291**, 553-561 (1998)). Thus it is reasonable that the plasticizer itself may influence the overall photorefractive performance. This idea has been confirmed in experiments in Germany, which investigated the importance of the choice of plasticizer on the photoelectric properties by comparing two materials that differ only in the plasticizers. (Hofmann, U.; Grasruck, M.; Leopold, A.; Schreiber, A.; Schloter, S.; Hohle, C.; Strohriegl, P.; Haarer, D.; Zilker, S. *J. J. Phys. Chem. B* **2000**, *104*, 3887.) The two plasticizers used in their study were N-(2-ethylhexyl)-N-(3-methylphenyl)-aniline (EHMPA) and dioctyl phthalate (DOP), which were observed to affect the dispersivity of charge transport. EHMPA worked much better than DOP due to better trapping. In our synthetic efforts, we synthesized the plasticizers shown in the following table with various HOMO energies and glass transition temperatures. In this initial series, the oxidation potential does not vary greatly, as all of the compounds are essentially derivatives of carbazole. This class of plasticizers would not be expected to add additional deep traps when used in PVK composites.

Chemical Structure	Tg (°C)	Mp (°C)	Eox*/HOMO
	NA	72	1.14 V -5.50 eV
	NA	68	1.14 V -5.50 eV
	Clear Liquid	Clear Liquid	1.14 V -5.50 eV
	13	153	1.09 V -5.45 eV
	-15	71	1.09 V -5.45 eV
	Clear Liquid	Clear Liquid	1.09 V -5.45 eV

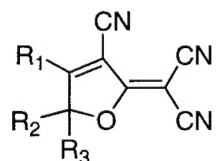
*CV: Pt electrode, Pt disk and Hg/HgCl₂/NaCl reference electrode, 0.1 M tetraethylammonium tetrafluoroborate in acetonitrile as supporting electrolyte, speed: 300 mV/sec.

C. Synthetic Efforts: Charge transporting polymers

In our workhorse PVK/AODCST/BBP/C60 material, there is always some type of unwanted photochromism after a few hours of optical irradiation under electric field. In other words, a differently colored spot occurs after some time. From the electrochemistry of each component, we found that the monomer of PVK (ethyl carbazole) gave irreversible first anodic sweep in CV measurements. Its second anodic sweep gave an extra reversible process at a lower voltage, which can be attributed to the dimer of ethyl carbazole. This means that after losing one electron, the PVK monomer cation tends to be rather reactive and can couple with itself at least at solution conditions. It is not known if this effect is occurring in the solid PVK-based composites. Nevertheless, we decided to prepare two PVK derivatives as shown below to increase the steric hindrance of the reactive sites and thus protect them, which are the carbons para to the nitrogen, by inserting some electrochemically stable groups. In our synthetic efforts, the tert-butyl protecting group was chosen first due to synthetic accessibilities.

	PVK from Aldrich		
Mw	109984	94104	71462
Mn	46417	38776	25389
Mw/Mn	2.369	2.425	2.815
Tg (°C)	180	273	254

D. Synthetic efforts: New NLO chromophores based on the 2-dicyanomethylen-3-cyano-2,5-dihydrofuran (DCDHF) acceptor.



R1: electron donating group

R2, R3: can be adjusted to tune the ancillary physical properties of the chromophore.

In some recent publications (Zhang, C.; Ren, A. S.; Wang, F.; Zhu, J.; Dalton, L. R.; Woodford, J. N.; Wang C. H. *Chem. Mater.* **1999**, *11*, 8, 1966; Dalton, L. R. et al. *J. Mater. Chem.* **1999**, *9*, 1905; Robinson, B. H.; Dalton, L. R. et al. *Chemical Physics* **1999**, *245*, 35; Zhang, C.; Wang, C.; Yang, J.; Dalton, L. R.; Sun, G.; Zhang, H.; Steier, H. *Macromolecules* **2001**, *34*, 235), the electron accepting 2-dicyanomethylen-3-cyano-2,5-dihydrofuran (DCDHF) ring has been incorporated into a conjugated system to make electrooptic materials with exceptional hyperpolarizability. However, the use of this functional group in organic photorefractive materials has not been explored. One of the advantages of this structure is that various electron-donating groups can be placed at R1, and R2, R3 can be adjusted to tune the ancillary physical properties of the chromophore. In particular, it is possible to get a glassy monolithic photorefractive material. In our synthetic efforts, we have synthesized a series of DCDHF containing chromophores with and without an olefin link between the electron donating part and the electron accepting part of the molecule. The dyes with olefinic connectivities have longer absorption wavelength and a site of possible instability (even if endocyclic and heterocyclic). In addition, the dyes are often insoluble and have high melting points. On the other hand, the dyes containing no free olefinic components have shorter absorption wavelength and better solubility. In addition, there is no concern about photochromic gratings in these molecules, so they may be more suitable for photorefractive

studies. The following table shows the molecules synthesized so far. These new molecules provide a rich novel class of chromophores for photorefractive polymer materials.

	λ_{max} (nm) (THF)	Mp (DSC) ($^{\circ}\text{C}$)	Td (TGA) ($^{\circ}\text{C}$)	$*E_{1/2}^{\text{ox}}$ (V) / HOMO (eV)
	572	188	210	0.96 -5.32
	561	212	278	0.98 -5.34
	539	331	336(at mp)	1.093 -5.45
	483	>278	278(at mp)	Insol
	486	184	312	1.28 -5.63
	491	127($T_g = 15^{\circ}\text{C}$)	320	1.21 -5.56
	492	171($T_g = 10^{\circ}\text{C}$)	312	1.22 -5.57
	492	140($T_g = 30^{\circ}\text{C}$)	318	1.19 -5.54

* CV: Pt electrode, Pt disk and Hg/HgCl₂/NaCl reference electrode, 0.1 M tetraethylammonium tetrafluoroborate in acetonitrile as supporting electrolyte, speed: 300 mV/sec.

E. Physical Studies: New charge-transporting host polymers based on poly(siloxane)

Most photorefractive polymer (PRP) composites have used poly(n-vinyl carbazole) (PVK) as the polymer matrix and charge transporting medium. PVK has many advantages, including its commercial availability, the depth of study on the polymer, and its ability to dissolve polar chromophores. Almost all the progress in the field has been accomplished with materials using this polymer, but PVK also has several disadvantages. In light of the discovery of the “orientational enhancement” effect, there is much to be gained in terms of index contrast if the T_g of the composite is close to room temperature. Unfortunately, the intrinsic T_g of PVK is above 200 C, and an additional plasticizer must be added. The addition of plasticizer can be deleterious since it wastes volume in the sample, can lead to phase separation, and can effect the PR dynamics, often in ways that are difficult to understand. We sought to solve

several of the above problems simultaneously by characterizing the following polymers synthesized by Mike DeClue and Prof. Jay Siegel, UCSD:

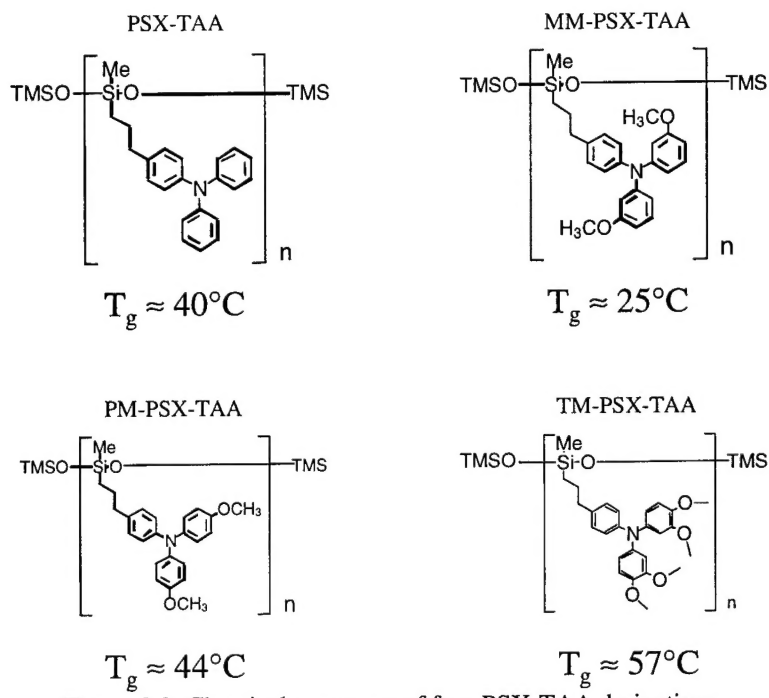
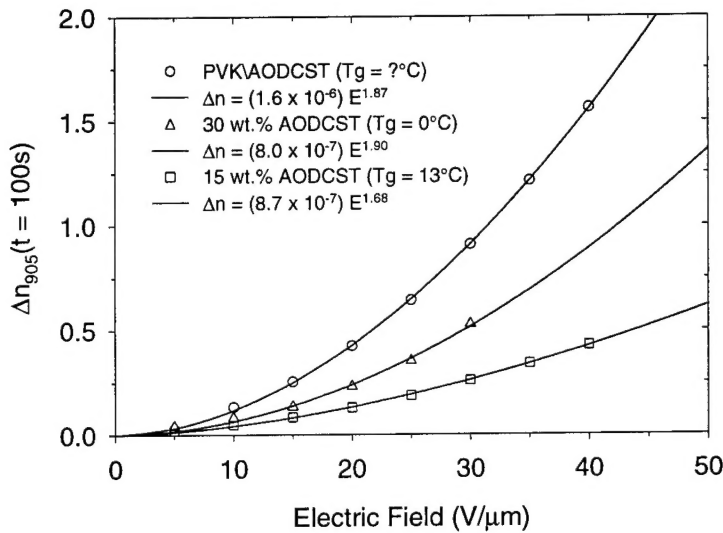


Figure 2.2: Chemical structures of four PSX-TAA derivatives

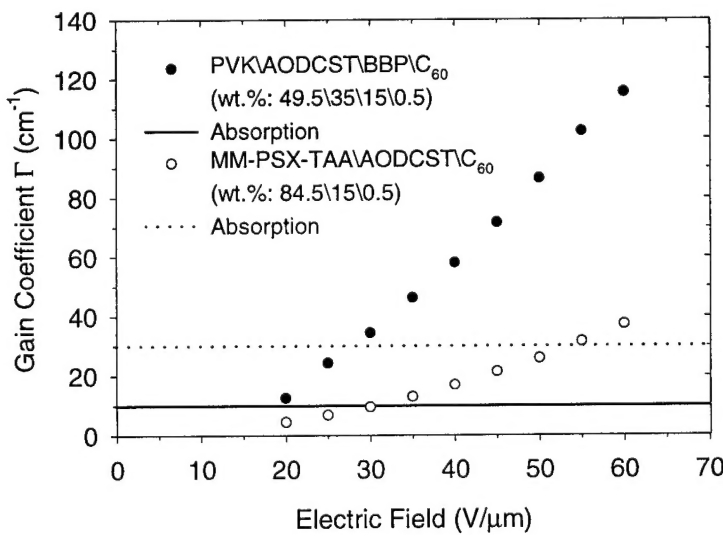
As one can see, the poly(siloxane) backbone has a much lower T_g than that of PVK. The xerographic community has studied the tris-tolylamine (TTA) monomer, and when doped into polystyrene, mobilities up to $10^4 \text{ cm}^2/\text{Vs}$ have been measured. TTA also has a lower oxidation potential than carbazole. Thus this combination of a better charge transport agent with a polymer that does not require additional plasticizer could lead to an improved composite. The additional methoxy groups were added to improve the solubility of polar chromophores in the matrix. We were able to make composites with these materials without any additional plasticizer. The best results were obtained with composites of MM-PSX-TAA\AODCSTC₆₀, which are described below.

Transient ellipsometry is a technique commonly used to probe the orientational dynamics of chromophore in PR polymers. The technique can allow one to sense the time dependence and magnitude of the refractive index change created by the poling of the chromophores by an external electric field. These experiments were used to quantify the orientational characteristics of the chromophores in the new composite. The quasi steady state results (after 100 seconds) are shown below.



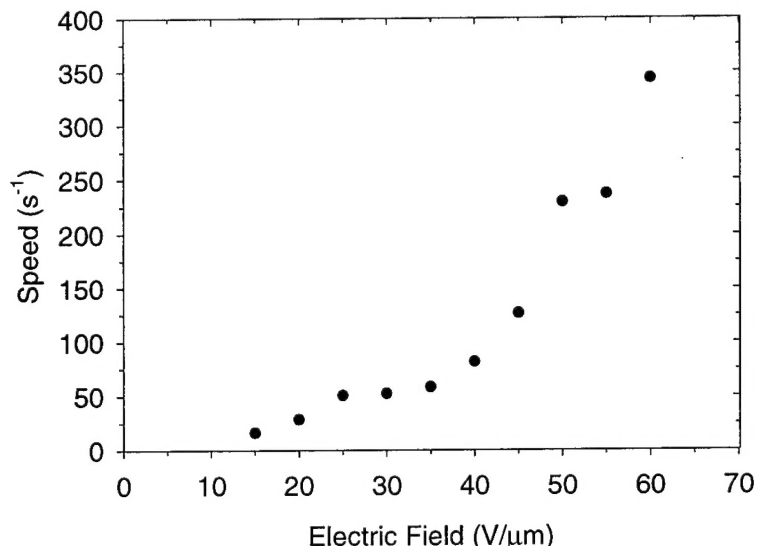
Electric field dependence of the quasi steady state refractive index change.

In this figure we compare the electric field dependence of the refractive index change in samples of PVK\AODCST\BBP\C₆₀ (49.5\35\15\0.5 wt. %, upper curve, where BBP is butylbenzylphthalate), MM-PSX-TAA\AODCST\C₆₀ (69.5\30\0.5 wt. %, middle curve), and MM-PSX-TAA\AODCST\C₆₀ (84.5\15\0.5 wt. %, lower curve). As can be seen in this figure, there is a reduction of the quasi-steady-state magnitude of the nonlinearity by about a factor of two between the PVK composite and the PSX material, even though the wt. % of the chromophore is the nearly the same, and about a factor of three when we use 15 wt. % of AODCST. We can only conclude that the difference is due to AODCST occupying a smaller volume fraction in the PSX-TAA composite. We also observe a factor of three difference in the non-linearity between PVK\AODCST\BBP\C₆₀ and MM-PSX-TAA\AODCST\C₆₀ (84.5\15\0.5 wt. %) when comparing steady-state refractive index changes measured by four wave mixing (FWM) (data not shown) and in the steady-state gain coefficients in two wave mixing (TWM) experiments:



TWM gain coefficient comparison of PSX-TAA and PVK samples

When we compare the speeds of the PSX-TAA and PVK composites, the PSX-TAA composite has about a factor of three larger speed at equivalent experimental conditions. As can be seen in figure below, average speeds of several hundred inverse seconds can be obtained at fields below 60 V/ μ m:

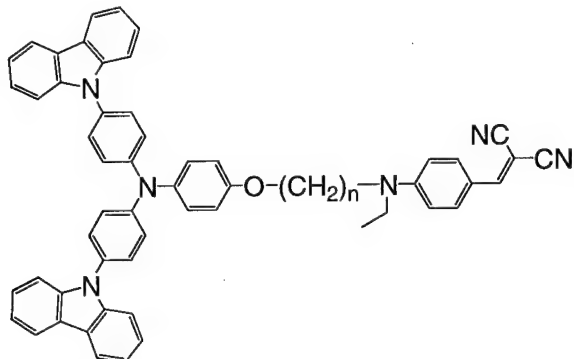


Averaged photorefractive speed comparison of MM-PSX-TAA\AODCST\C₆₀ vs. applied electric field at a writing intensity of 1 W/cm².

In conclusion, these new polymers have several attractive features as compared to the standard PVK, including no need for additional plasticizers and possibly higher hole mobility. We observe a reduction of non-linearity when using the chromophore AODCST, probably due to reduced volume fraction of the chromophore in the PSX-TAA samples. The photorefractive speed was similar to the best one can achieve with PVK composites, which puts the new PSX-TAA among those PRP polymer materials with the highest speeds reported to date.

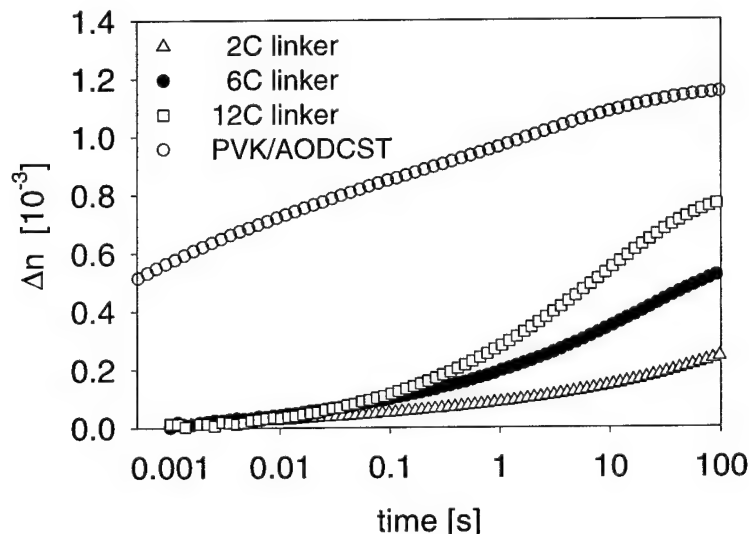
F. Physical Studies: Photorefractive characterization of NLO-DCTA monomeric glasses

One of the stability issues with PRPs is that of shelf life. Guest/host composites often suffer from tradeoffs stemming from the polarity of the NLO chromophore. The crux of the problem is that the non-linearity of the chromophore increases with its dipole moment, but the miscibility of the molecule in the usually non-polar host polymer is reduced and phase separation or crystallization can occur. This often results in a choice between good PR performance and low shelf life stability, or good shelf life and poor performance. One approach to solve this problem is to use glass-forming molecules instead of polymeric composites.



General structure of DCTA-DCST glass forming molecules

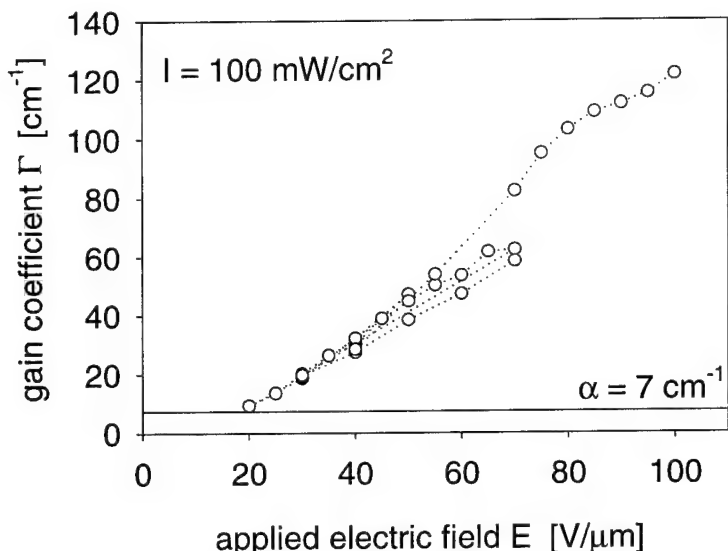
Following last year's work on dicarbazole triphenyl amine (DCTA) glasses, the Kent group has synthesized three different versions of the molecule depicted in the figure above, with n equal to 2, 6, and 12 carbon atoms. All molecules can be combined with C_{60} and the plasticizer DOP (35, 25, and 20 weight percent, respectively) to form glassy photorefractive films with T_g s near room temperature ($\sim 22^\circ\text{C}$). Transient ellipsometry experiments were used to quantify the orientational characteristics of the glasses. Samples of each glass plasticized to a T_g near 22°C were compared to a composite of PVK\AODCST\BBP\(C_{60} (described above):



Transient ellipsometry curves for samples of the three different DCTA-DCST glasses and a PVK\AODCST\BBP\(C_{60} composite at $30 \text{ V}/\mu\text{m}$.

As can be seen from the figure, the glasses orient on much longer time scales than the PVK\AODCST\BBP\(C_{60} composite. The orientation is quite dispersive, having dynamics observable over more than four orders of magnitude in time. We see an interesting trend in that the orientation of the chromophore in the glass samples seems to become faster as the length of the linker is increased, even though all the samples have the same T_g . We have also performed two wave mixing measurements on these glasses to assess their photorefractive parameters. The transient behavior suggests two time-dependent processes are active in this material, most likely space-charge field formation and chromophore orientation, and this

effect will be discussed in a forthcoming publication. Field-dependent measurements of the steady-state gain coefficient were performed on all the glasses, and the figure below shows the results for DCTA-12C-DCST/DOP/C₆₀

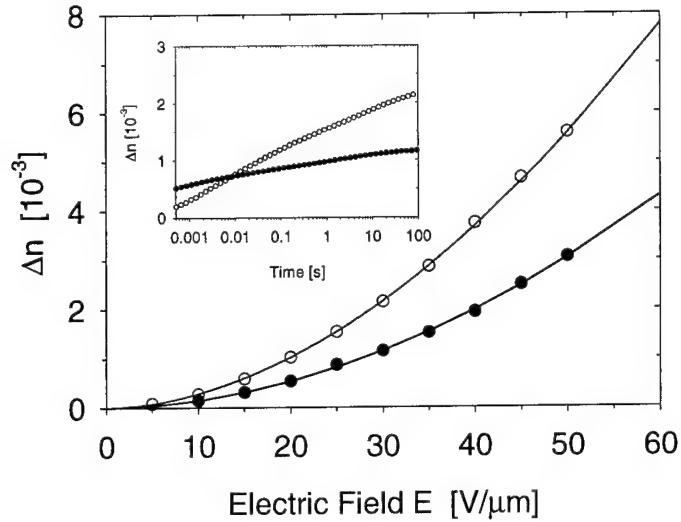


TWM gain coefficient versus applied electric field in DCTA-12C-DCST/DOP/C₆₀ at a total intensity of 100 mW/cm² and a wavelength of 676 nm. The absorption (α) is indicated by the dashed line. The dotted lines indicate the order of the measurements.

The gain coefficient is larger for samples made with the longer linker, which is what we expect from the ellipsometric data. We also expect these gain coefficients to be lower than that of PVK\AODCST\BBP\C₆₀ composites²⁴ which is the case. Due to the red-shifted absorption spectrum of DCTA-2C-DCST net gain is reached only for fields above 50-60 V/μm. In DCTA-12C-DCST net gain is already achieved at 20 V/μm as the absorption coefficient is only 7 cm⁻¹. Thus longer linkers are favorable due to larger dynamic range and improved optical clarity. In addition, the observed net gain coefficients (above 100 cm⁻¹) are quite respectable and suggest that this materials class deserves further development. However, the slight variations in gain coefficient which depend upon the order of the measurements suggest that hysteresis and memory effects are present in this material.

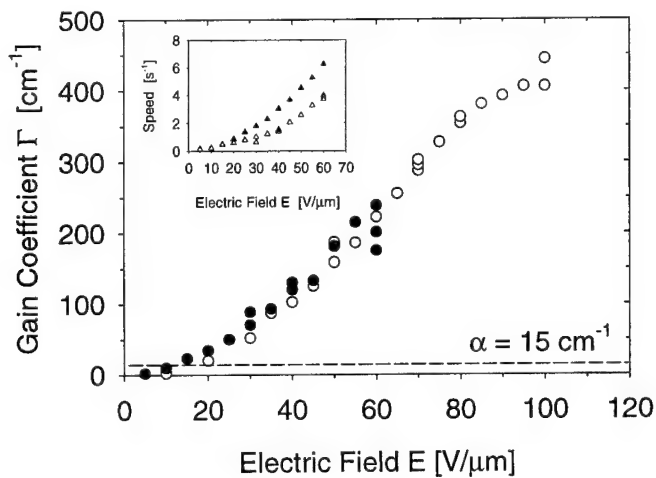
G. Physical studies: New composites and glasses based on DCDHF chromophores

A new non-linear optical chromophore for photorefractive applications containing a 2-dicyanomethylene-3-cyano-2,5-dihydrofuran acceptor group has been prepared by the synthetic collaborators at Kent State. When doped into a plasticized composite of poly(n-vinylcarbazole), large gain coefficients (Γ) are observed with photorefractive speed similar to the best composites reported in the literature while maintaining low sample absorption (~ 15 cm⁻¹). We focus here on the composite DCDHF-6, entry 6 in the table in Section D above.



Applied electric field dependence of the refractive index change 100 seconds after the field was applied in composites of DCDHF-6 (empty circles) and AODCST (filled circles). Fits described in text. Inset: Time evolution of the Δn for an applied field of 30 $\text{V}/\mu\text{m}$ for DCDHF-6 (empty circles) and AODCST (filled circles).

The performance of the samples in ellipsometry is quite good, with index changes larger than our model material occurring at all fields (see figure above). Most importantly, in TWM studies, gain coefficients up to 400 cm^{-1} were observed (see figure below)! The inset also shows that the speeds of the new material compare quite favorably with the model AODCST system. This is a crucially important result: not only does this newest composite based on DCDHF-6 show very high gain, it does so with speed comparable to the fastest composites. While many new materials show large gain, often the observed response is quite slow, and this is not the case here. Therefore, a number of new applications in optical signal processing may be enabled by this new material.



Applied electric field dependence of the gain coefficient for a composite sample of DCDHF-6 with high beam ratio (empty circles) and with beam ratio of unity (filled circles). Inset: Applied electric field dependence of the photorefractive speed at a writing intensity of $100 \text{ mW}/\text{cm}^2$ for DCDHF-6 (empty triangles) and AODCST (filled triangles).

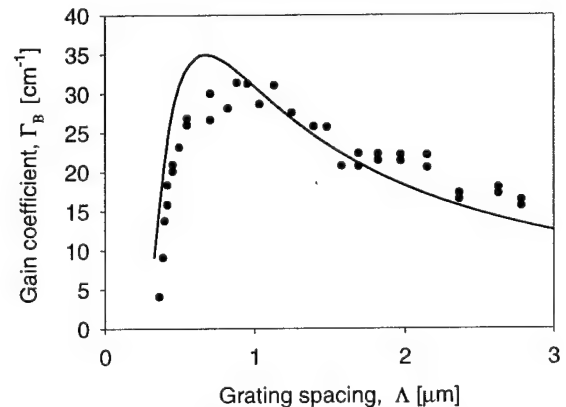
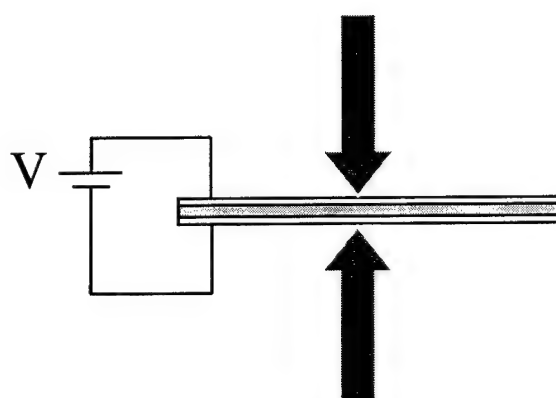
H. Physical Studies: Longitudinal geometries for polymer fiber applications in laser protection

The key issue in the use of PR polymers in a fiber geometry is to determine the actual optical geometry and applied field direction used to achieve beam coupling and/or beam suppression. Once this is determined, issues of material type and characteristics will be easier to analyze. We have analyzed the following configurations in a report sent to Dr. C-Y Lee and Prof. M. Kuzyk:

(a) Opposite side geometry, longitudinal applied field

This configuration is closest to that commonly used to study beam coupling effects in PR polymers, so a reminder of what has already been observed in this regime is a good starting point. The sample is typically a plate ~ 100 microns in thickness, and the electric field is applied in the longitudinal direction, perpendicular to the sample plane as shown below. This configuration demands the highest wavevector response from the sample (or the shortest grating period). The beam-coupling gain coefficient versus grating spacing for our PVK:PDCST:BBP:C₆₀ material was published in *JOSA B* **15**, 905-913 (1998) as shown below on the right with an applied field of 41 V/micron.

The counterpropagating geometry is the point shown at the smallest grating spacing. It is clear that the counterpropagating geometry really works; however, the coupling coefficient is smaller than at other crossing angles due to the value of the trap density. The peak in the curve shown would shift to the left with higher trap density, which could possibly be achieved by doping the sample. Our current research into trapping physics directly addresses this problem.

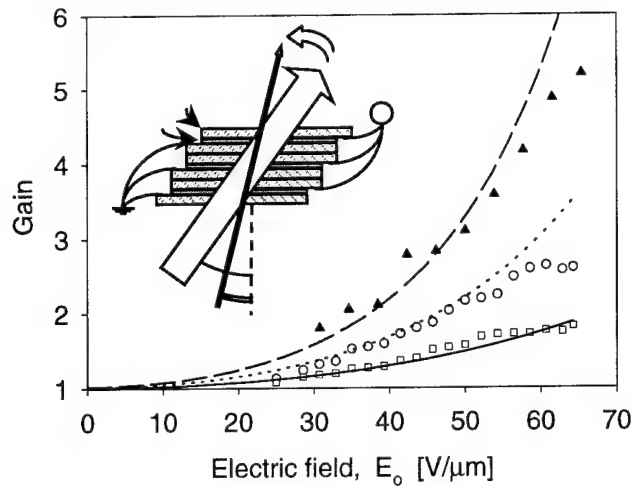


However, the most serious problem with this geometry in a fiber configuration is the difficulty of achieving high fields along the fiber axis, or across a thick plate sample.

(b) Multilayer geometry to achieve high gain and high applied field

One solution to both the small gain factor of part (a) and the challenge of applying the field, would be to use **multilayer stacks**, as we described in *Science* **277**, 549-552 (1997), as shown in the diagram below. This configuration would also work in the counterpropagating geometry. In this geometry, there is no fiber, and no need for waveguide propagation. Multiple stacks provide

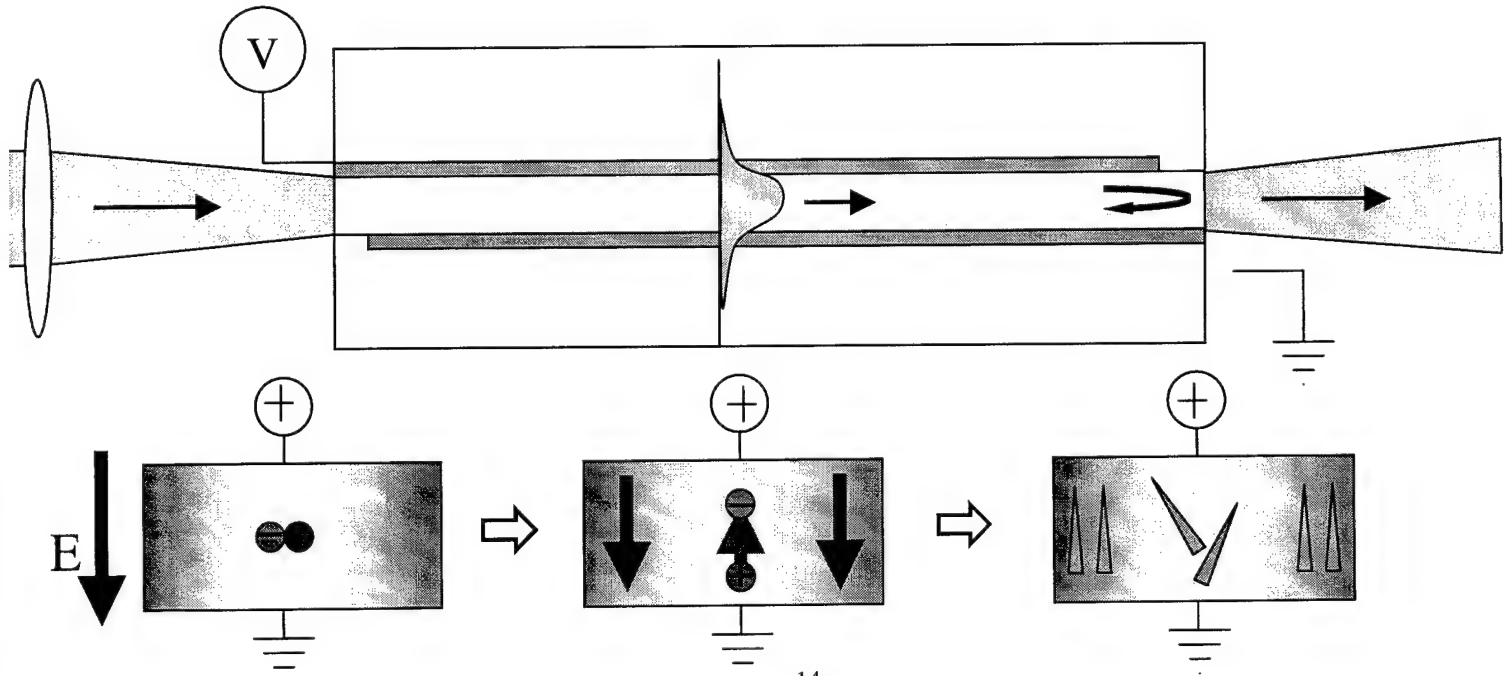
an increase in gain given by the product of the gain factors for each slice. The stack need not be placed at a focus in the optical system.



With this approach, the critical issues would be the engineering problems of fabricating the multilayer stack, designing ITO coatings on both sides of glass plates, electrode connections, etc. It would still be critical to increase the trap density in order to maintain the number of layers at a manageable level.

(c) Fiber geometry with transverse applied field

We considered in some detail the transverse geometry for PR polymers as a possible laser protection device. The basic geometry looks like the upper part of the figure below, where the light travels down a long optical waveguide or fiber, across which an electric field is applied. The operation would be as follows: with one laser beam incident, a backreflected beam coming from scattering or a partial mirror at the output might be amplified by beam coupling, thus suppressing and depleting the transmitted beam.

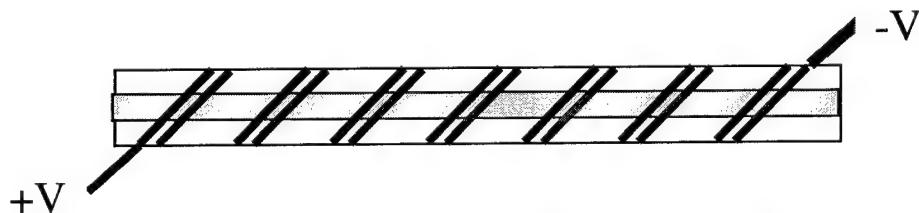


The microscopic picture of what might happen is shown in the bottom three images. The forward and backward beams produce a standing wave intensity pattern. Assuming blocking electrodes, the photoconductivity in the bright regions generates an internal field that screens part of the applied field, producing an index modulation along the axis of the waveguide. For an orientational material, the order parameter would be reduced in the region of screened field.

While producing a sample in this configuration would be possible in principle using Kuzyk's methods of embedding electrodes in pulled polymer fibers, **unfortunately this configuration should not produce strong beam coupling.** We have verified this theoretically and experimentally. The regions of index modulation are exactly in phase with the optical standing wave, so no coupling between the forward and backward waves would occur.

(d) New Proposed Fiber Geometry #1: Spiral electrodes

One geometry which might produce a longitudinal field in a fiber geometry is shown below. The basic scheme is to produce a longitudinal field in order to achieve a nonzero phase shift by the usual photorefractive effect. We imagine a small-diameter capillary which can be filled with the PR polymer composite at a high temperature by capillary action, and then cooled to room temperature. Then a pair of wire electrodes could be wound around the capillary with uneven spacing. This should produce fringing fields in the core of the capillary which are stronger along one longitudinal direction than the other, e.g., a larger field along $+z$ compared to $-z$.



This geometry may present a challenge in the fabrication, but this does not seem fundamental at this point. Calculations of the field at the center would be helpful in estimating the size of the longitudinal field that can be achieved.

(e) New Proposed Fiber Geometry #2: Longitudinal field achieved with Hall effect

A second idea we have generated is to use a transverse E field as in (c) above along with a longitudinal **magnetic** field, produced either by a solenoidal winding around the fiber, or by a pair of Helmholtz coils. In this case, the Hall effect would produce charge motion partially along the axis of the structure, resulting in a longitudinal space charge field. Issues for this geometry include limitations due to charge mobility, the size of the B field that can be produced, what phase shift would be obtained, etc.

Both of the new geometries proposed in (d) and (e) above are completely new to our knowledge. Much is unknown about these configurations in terms of tradeoffs and implications for the materials design.

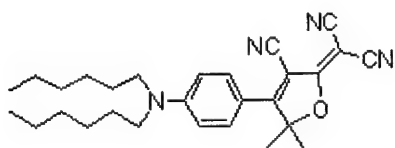
I. Year Three Physical/Optical Studies:

(a) Photochromic Polymers for the Optical Homodyne Detection of Ultrasonic Surface Displacements

We have developed a novel scheme to detect small ultrasonic surface displacements using a photochromic polymer instead of a photorefractive material as an adaptive beam combiner in a two-wave mixing geometry. Poly(methylmethacrylate) is doped with a derivative of zinc-tetrabenzoporphyrin possessing a long lived triplet state which can be efficiently populated in a reversible manner. The resulting dynamic hologram consists of local absorption and refractive index gratings, which can process speckled beams reflected from rough surfaces. We believe that this is the first use of a local nonlinear medium for adaptive homodyne detection of ultrasonic surface displacements. U. Gubler, D. Wright, W. E. Moerner, and M. B. Klein, "Photochromic Polymers for the Optical Homodyne Detection of Ultrasonic Surface Displacements," *Opt. Lett.* **27**, 354-356 (2002).

(b) Monolithic Photorefractive Organic Glasses with Large Coupling Gain and Strong Beam Fanning

The study of photorefractive materials has been driven in the past three decades by potential applications including data storage and optical processing based on transient, dynamic holograms. After the first two decades of research dominated by inorganic insulating crystals, the photorefractive effect was also discovered in semiconductors, organic crystals, polymers, and liquid crystals. In photorefractive polymer composites, various chemical species are combined as dopants in a host polymer to enable the different sub-processes necessary for the photorefractive effect. This low-cost and easy-to-process scheme offers great flexibility to change the photorefractive properties by modifying the various ingredients. An alternative approach with the same advantages and providing a higher concentration of the nonlinear optical moiety involves the use of a monolithic (single-component, but multifunctional) glass-forming molecule instead of the host-guest approach. This glass-forming molecule should simultaneously enable macroscopic charge generation and transport, provide optical nonlinearity and must be stable under illumination and high electric fields. As the dominant nonlinear response in this type of material stems from the anisotropy of the molecular polarizability, the glass transition temperature of the glass has to be close to room temperature to allow dynamic reorientation of the chromophores. We present in this work a new monolithic glass based on the novel chromophore DCDHF-6 (structure below), which possesses all of the above requirements and exhibits large photorefractive gain coefficients at moderate applied electric fields. U. Gubler, M. He, D. Wright, Y. Roh, R. J. Twieg, and W. E. Moerner, "Monolithic Photorefractive Organic Glasses with Large Coupling Gain and Strong Beam Fanning," *Adv. Mater.* **14**, 313-317 (2002).



(c) Monolithic Photorefractive Organic Glasses with Large Coupling Gain: Detailed Measurement of Photoconductive, Orientational, and Photorefractive Properties at Room Temperature

The photoconductive, orientational and photorefractive properties of several monolithic glasses based on new non-linear optical chromophores containing a 2-dicyanomethylene-3-cyano-2,5-dihydrofuran (DCDHF) acceptor group have been measured. Large net gain coefficients are observed in both red and infrared wavelength regions. The physical and optical properties of glasses based on various DCDHF-containing derivatives are compared and analyzed, and the factors limiting steady-state and dynamical photorefractive performance are discussed. Key in these materials is the relatively slow response produced by sluggish orientational alignment of the materials, which has been circumvented in temperature dependent studies (see below). O. Ostroverkhova, D. Wright, U. Gubler, W. E. Moerner, M. He, A. Sastre-Santos, R. J. Twieg, "Recent Advances in the Understanding and Development of Photorefractive Polymers and Glasses," *Adv. Func. Mater.* **12**, 621-629 (2002).

(d) High-Performance Photorefractive Organic Glass with Near-Infrared Sensitivity

A new organic glass mixture comprised of two dicyanohydrofuran (DCDHF) derivatives is presented. A pronounced two-beam coupling effect was observed at a wavelength of 830 nm in an unsensitized composition. Sensitization with TNFM led to a significant increase in two-beam coupling gain coefficient, reaching a net value of $\sim 370 \text{ cm}^{-1}$ at an electric field of 45 V/ μm at 1% TNFM, and resulted in an improvement in photorefractive speed. O. Ostroverkhova, W. E. Moerner, "High-Performance Photorefractive Organic Glass with Near-Infrared Sensitivity," submitted to *Appl. Phys. Lett.* (2002).

(e) New Fluorophores for Single-Molecule Spectroscopy

We have discovered a new class of fluorophores that can be imaged at the single-molecule level and offer additional beneficial properties such as a significant ground state dipole moment μ_g , moderate hyperpolarizability and viscosity-dependent fluorescence. These molecules contain an amine donor and a dicyanodihydrofuran (DCDHF) acceptor linked by a conjugated unit (benzene, thiophene, alkene, styrene, etc.) and were originally designed to deliver both high polarizability anisotropy and μ_g as nonlinear optical chromophores for photorefractive polymer/glass applications. Surprisingly, these molecules are also well-suited for single-molecule fluorescence applications. We have measured the bulk (ensemble) and single-molecule photophysical properties for several examples in this new class of single-molecule reporters. K. Willets, O. Ostroverkhova, M. He, R. J. Twieg, and W. E. Moerner, "New Fluorophores for Single-Molecule Spectroscopy," *J. Amer. Chem. Soc.* (appearing 2003).

(f) Role of Temperature in Controlling Performance of Organic Photorefractive Glasses

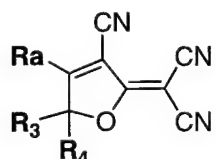
We have completed a detailed temperature dependence study of dielectric, birefringent, conductive and photorefractive (PR) properties of high performance low molecular weight organic glasses, containing dicyanodihydrofuran (DCDHF) derivatives. DCDHF organic

glasses sensitized with C_{60} exhibit high two beam coupling gain coefficients in the red wavelength region. However, in the best performing DCDHF glasses at room temperature, the PR dynamics are limited by slow molecular reorientation in the electric field. While orientational and, therefore, PR speed can be significantly improved with increasing the temperature above the glass transition temperature of the material, the steady-state performance may worsen. Comprehensive study of the temperature dependence of various processes contributing to the PR effect in DCDHF glasses clarifies the limiting factors and allows for optimization of the overall PR performance. O. Ostroverkhova, M. He, R. J. Twieg, and W. E. Moerner, "Role of Temperature in Controlling Performance of Organic Photorefractive Glasses," submitted to *ChemPhysChem* (2002).

J. Year Three Synthetic Studies (For structures and structure numbers, see the Table appended at the end of this document.)

During the third year of the project virtually all of the synthetic effort was devoted to the design, synthesis and characterization of the so-called "DCDHF" chromophores. These materials all contain a common acceptor group, the dihydrofuran heterocycle functionalized with a cyano group and a dicyanomethylene group. Additional dihydrofuran functionalization occurs at C_5 (R_3 and R_4) and eventual attachment to the rest of the chromophore is at R_a . R_3 and R_4 may or may not be identical and neither R_3 nor R_4 is hydrogen.

Chart. General structure of 2-dicyanomethylen-3-cyano-2,5-dihydrofuran (DCDHF) acceptor



R_a : conjugated and electron donating group

R_3, R_4 : can be adjusted to tune the ancillary physical properties of the chromophore.

The more complete structure of the DCDHF dyes is seen below. Systematic variations in R_1 , R_2 , Ar and n (in addition to R_3 and R_4 already mentioned) provide a wide range of overall electronic, optical and morphological properties.

Chart. General structure components of a complete DCDHF chromophore

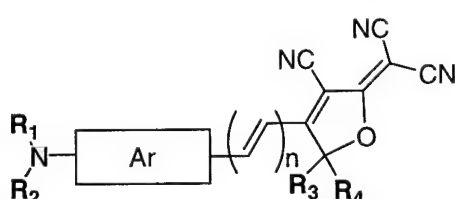
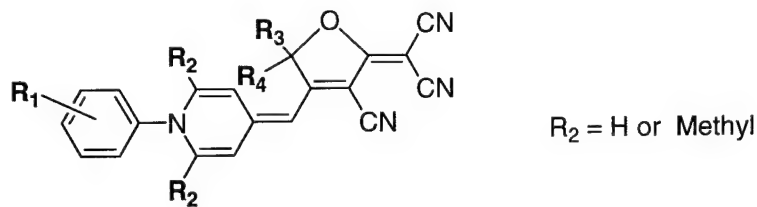


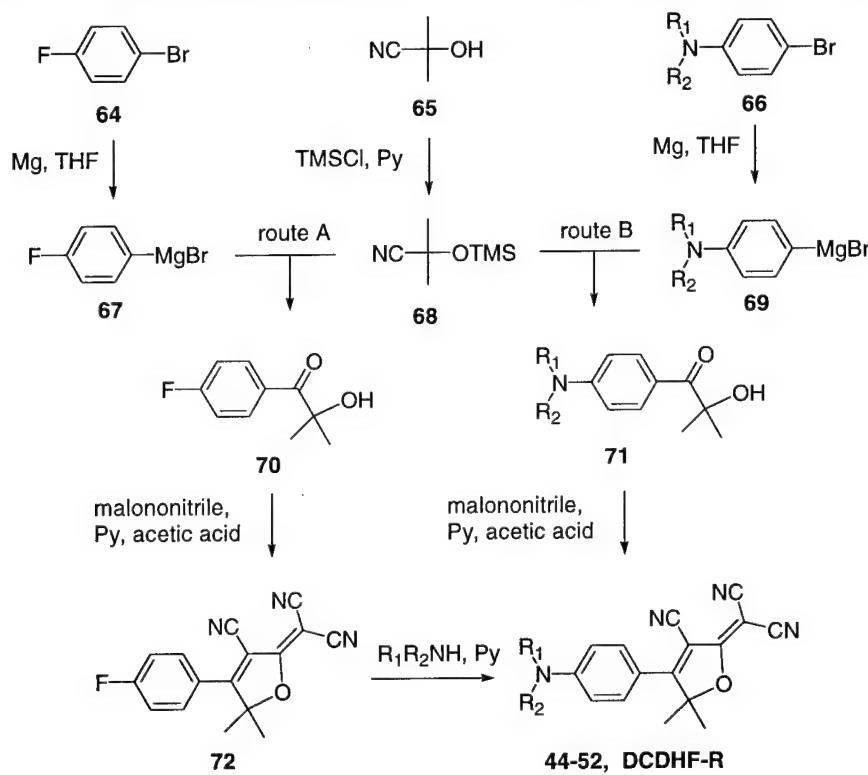
Chart. A special subset of DCDHF chromophores contain a dihydropyridine ring



The synthetic sequence utilized for individual DCDHF dyes is highly dependent on the structure of the specific overall chromophore. That is, the identity of any or all of the variables R_1 , R_2 , Ar, N, R_3 and R_4 may dictate the success of one route versus another. In the synthetic studies undertaken here one of the main overall accomplishments was the establishment of the different productive pathways leading to these compounds.

In the most simple systems with benzene attached directly to the heterocycle a route proceeding via an α -hydroxyketone produced from reaction of a Grignard reagent and a protected cyanohydrin and introduction of the amine last by aromatic nucleophilic substitution was generally the most productive. This route is shown below in Scheme 1.

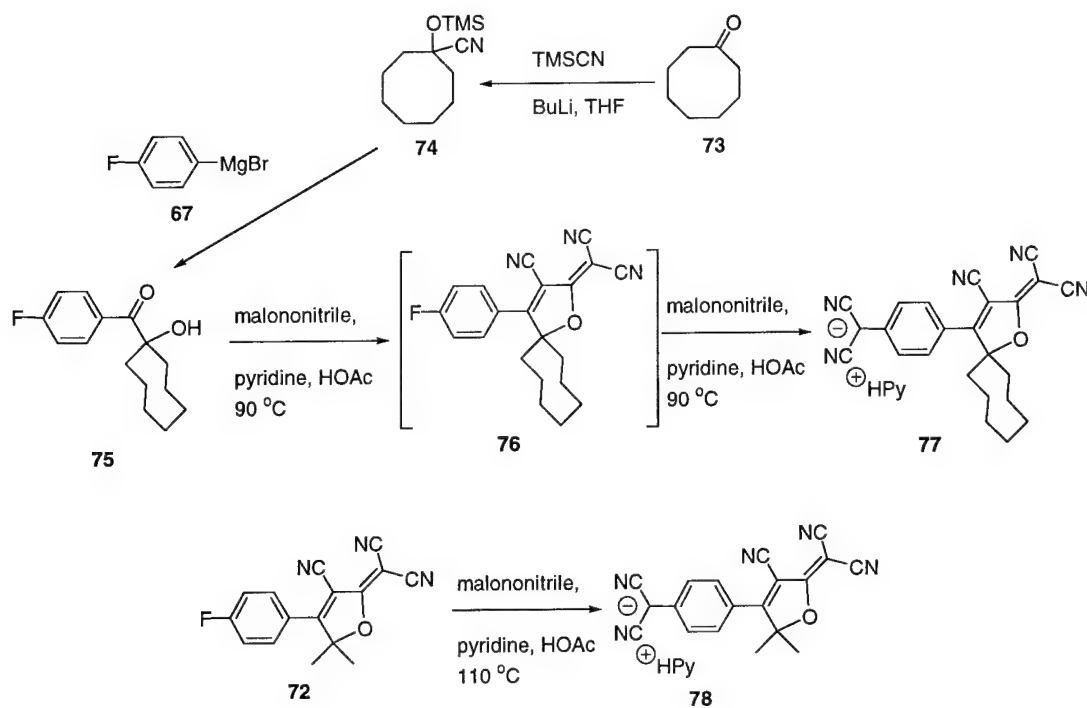
Scheme 1. The synthesis of chromophores 44-51 (Ar = Ph, n = 0, $R_3 = R_4 = CH_3$)



The route outlined in Scheme 1 worked well if R_3 and R_4 are small in size (e.g., methyl groups). However, when these two substituents on the precursor α -hydroxy ketone are sterically demanding and the heterocycle forming reaction is slow and must be run under forcing conditions problems occur. At the elevated temperature required to drive the heterocycle formation the desired aryl fluoride intermediate cannot be isolated due to an

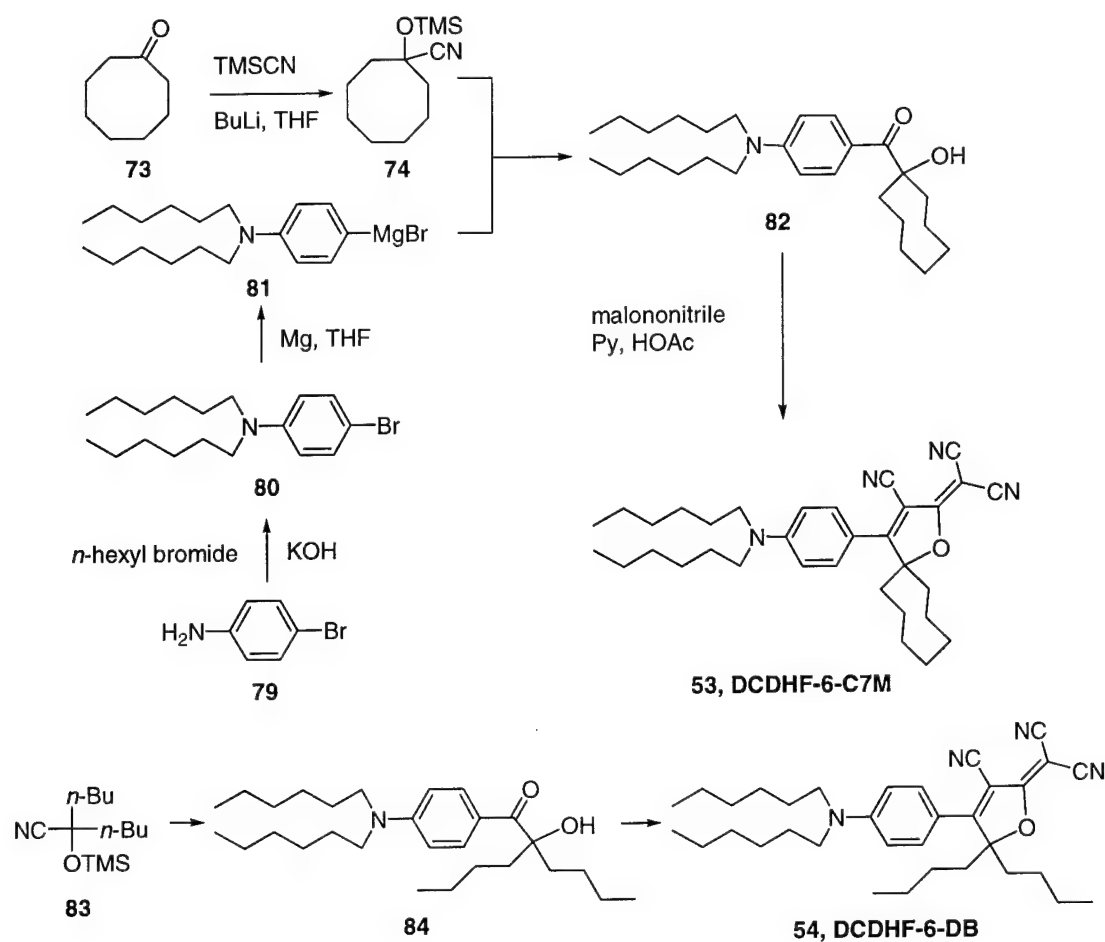
additional reaction with malononitrile (Scheme 2). This side reaction was substantiated by independent reaction with an isolated fluoroaromatic.

Scheme 2. Formation of malononitrile containing byproducts involving nucleophilic aromatic substitution by malononitrile on the aryl fluoride.



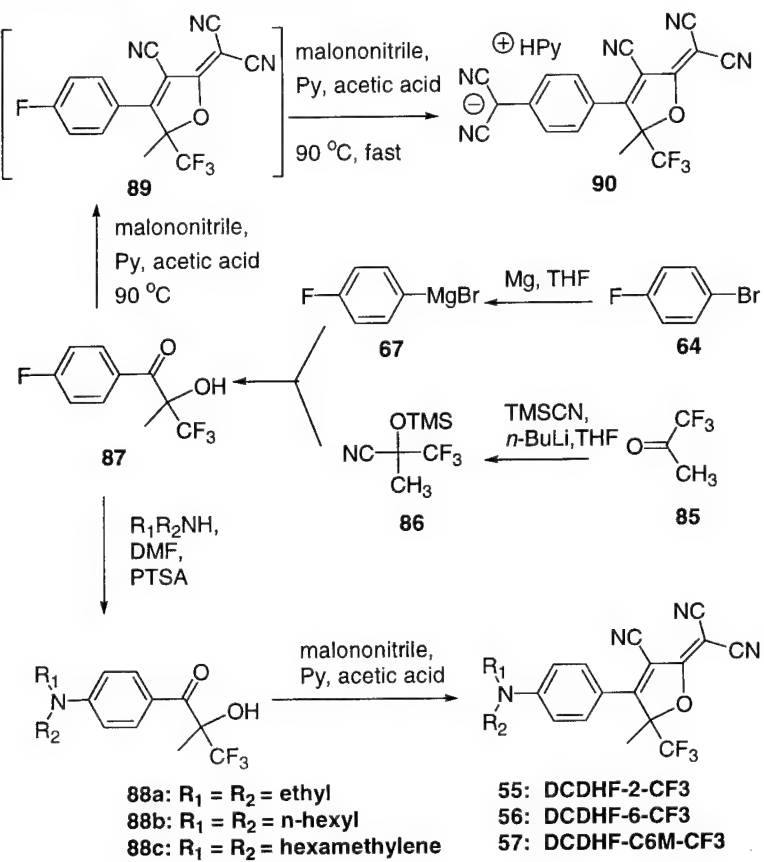
The problems in synthesis encountered due to large R_3 and R_4 groups were overcome simply by reversing the order of the synthetic steps. The revised synthesis wherein the amine was introduced prior to the heterocycle formation is shown in Scheme 3. Here the Grignard reagent already contains the amine group (instead of a fluorine).

Scheme 3. The synthesis of chromophores 53 and 54 containing bulky groups at R₃ and R₄



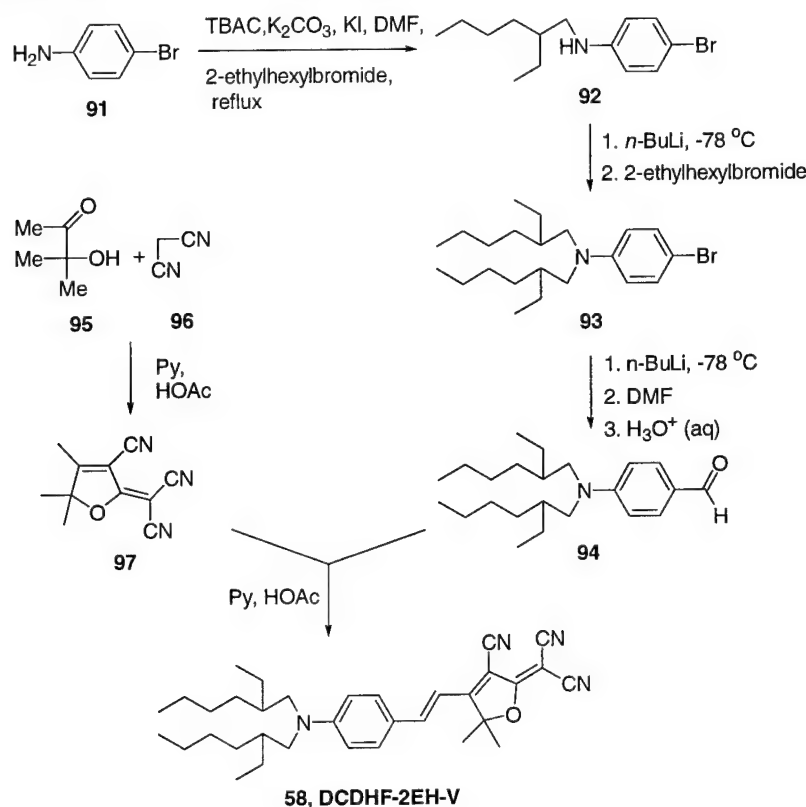
In the preceding cases the R₃ and R₄ groups are identical. Breaking this symmetry is a productive method to enhance the morphological properties of the dyes. This reduction in symmetry results simply from using an unsymmetrical ketone for creation of the cyanohydrin. A particularly interesting case that we have examined involves the use of 1,1,1-trifluoroacetone. Here the CF₃ group not only breaks the symmetry of the acceptor but also the inductive effect of the CF₃ group is manifested in different electronic and optical properties of the dye. For example, aromatic nucleophilic substitution of the amine on the fluoroaromatic with the additional trifluoromethyl group is now quite facile.

Scheme 4. Synthesis of Chromophores 55, 56 and 57 with fluorinated acceptor



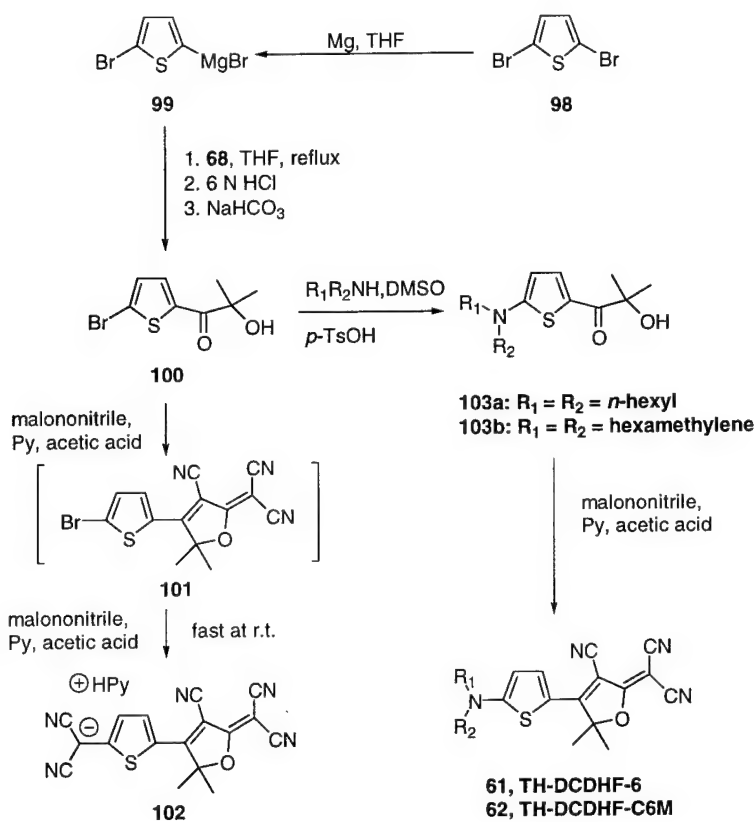
There is significant flexibility available in the choice of tails on the amine donor in these DCDHF chromophores. The use of relatively large tails is required to enhance the solubility of these materials and to adjust the melting and glass forming properties. In Scheme 5 is shown the chemistry developed for the introduction of a pair of 2-ethylhexyl groups. While this design looked attractive on paper it turned out that this extent of modification is not required, i.e., simple *n*-alkyl tails of medium length (hexyl, octyl) are able to provide sufficient glass-forming capability.

Scheme 5. Synthesis of DCDHF chromophore 58 with 2-ethylhexyl substituted donor



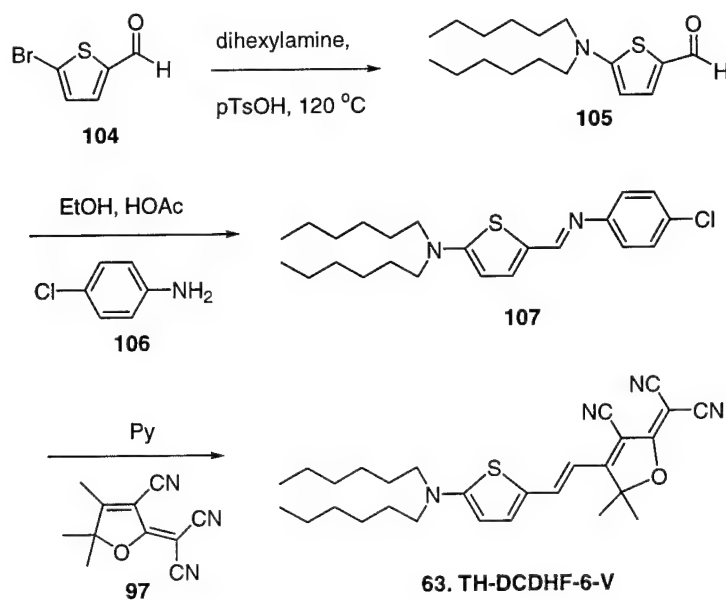
The substitution of thiophene for benzene in the DCDHF dyes with direct link to the acceptor heterocycle necessitated still further adjustments in the synthetic sequence. Here the most successful order of events shown in Scheme 6 includes creation of the α -hydroxyketone, aromatic nucleophilic substitution on the α -hydroxyketone and finally conversion to the heterocyclic acceptor. Unlike the case of the analogous benzene compounds (Scheme 1) here it proved impossible to isolate the desired halogen substituted precursor to general aromatic nucleophilic substitution.

Scheme 6. Synthesis of thiophene containing DCDHFs without an olefinic link



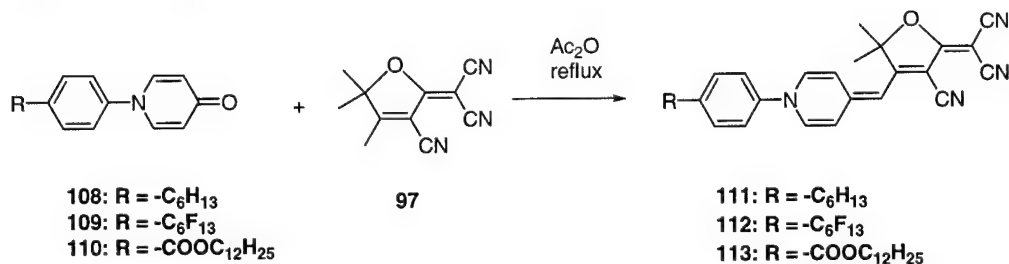
Adjustments in the linking olefins (variable examined here is limited to $n = 0$ to 1) are important to tune the electronic and optical properties. Simple systems with an alkene between an amine substituted benzene ring and the dihydrofuran acceptor group are easily prepared by a simple Knoevenagel condensation. However, this approach did not work for the analogous thiophene materials. In this case the adoption of the Siegrist technique for alkene synthesis was critical. Here the aldehyde is first converted to the imine and then it is condensed with the active methylene compound instead of the aldehyde. As shown in Scheme 7, by this route thiophene containing DCDHF dyes with extended conjugation were successfully prepared.

Scheme 7. Synthesis of thiophene containing chromophore 63 with an olefinic link



We have also synthesized an unusual group of DCDHF chromophores in which the donor nitrogen is part of a heterocycle, i.e., the nitrogen is contained in a dihydropyridine (DHP) ring. We had previously examined the optical and electronic properties of methylene dihydropyridines with more conventional electron deficient methylene substituents (cyano, ester, etc.). In the case shown in Scheme 8 the analogous DCDHF materials were prepared with hydrogens on the DHP ring while in Scheme 9 the dyes have a pair of methyl groups on the DHP ring.

Scheme 8. Synthesis of DCDHF chromophores containing a H-substituted DHP ring



Scheme 9. Synthesis DCDHF chromophores containing a CH₃-substituted DHP ring

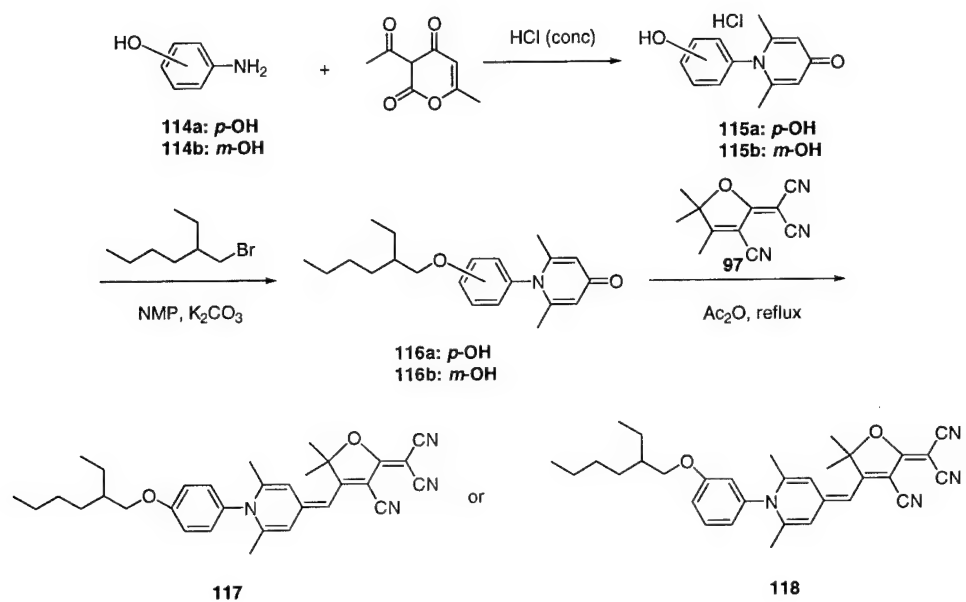


Figure 1. DSC traces of DCDHF-6 48 and Mix 1 (48 and DCDHF-6-C6M 53). In the top trace the melt is cooled and on rewarming a glass transition is seen followed by recrystallization and then followed by melting. In the bottom trace a mixture of dyes also shows a glass transition but in this case there is no evidence for recrystallization (evidence of enhanced glass stability).

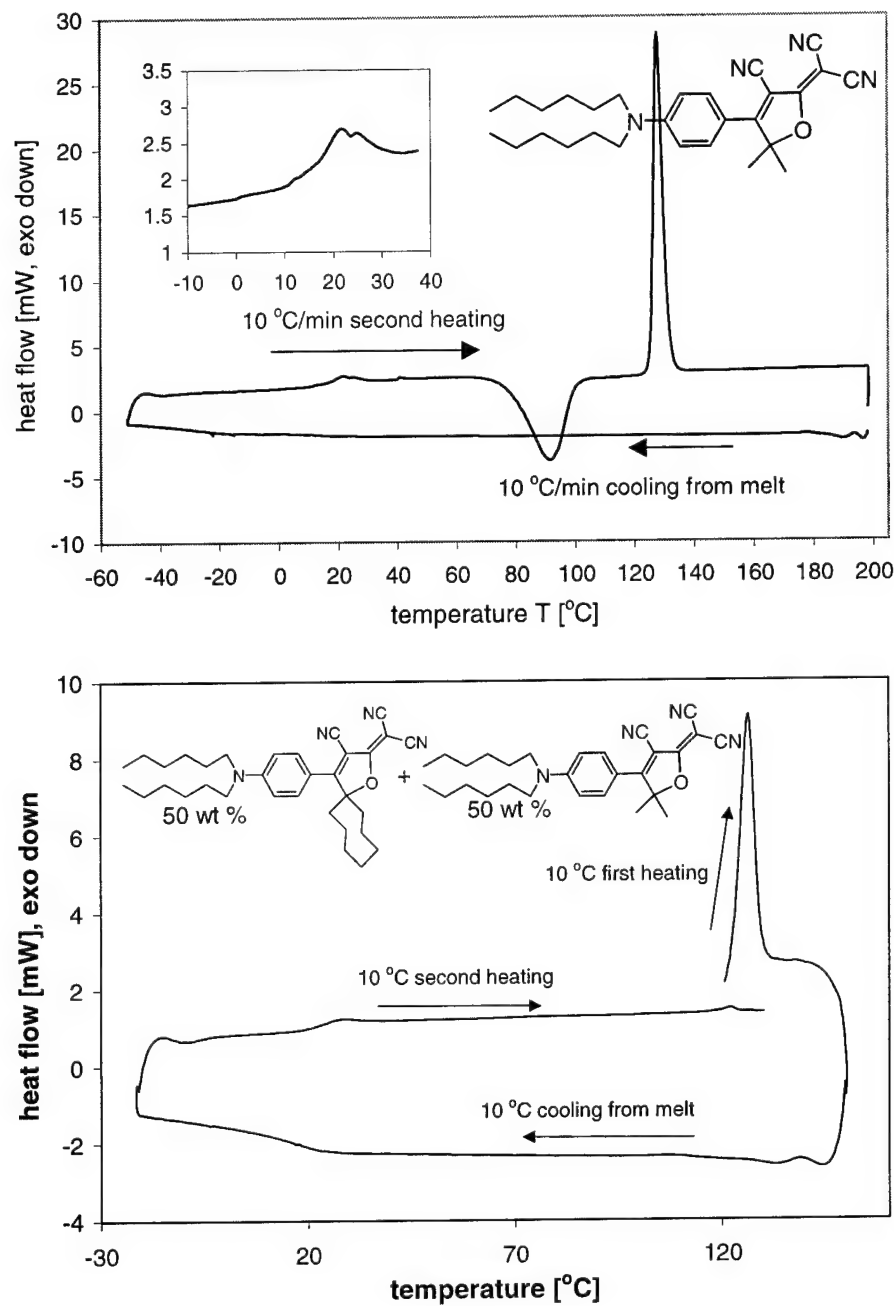


Figure 2. UV-Vis absorption spectra of some representative DCDHF dyes in THF. This figure shows how the charge transfer band is easily adjusted in energy by systematic changes in structure (see complete Table of structures for the identity of the specific compounds).

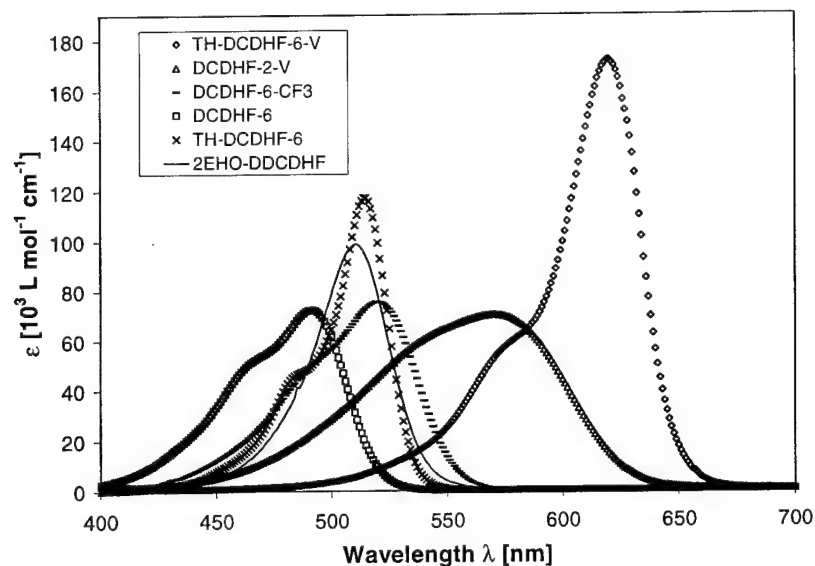


Figure 3. Concentration-dependent UV-Vis spectra of TH-DCDHF-6-V in CCl_4 . The arrows indicate the increase of concentration. The lower energy absorption is due to dimer.

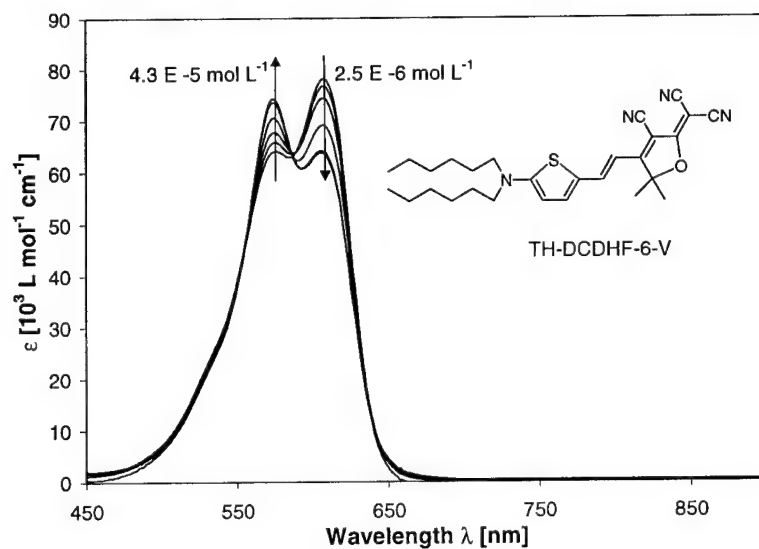


Figure 4. Solvatochromism studies of DCDHF-6 and TH-DCDHF-6. Neither of these dyes is particularly solvatochromic showing they are tuned for near optimal birefringence.

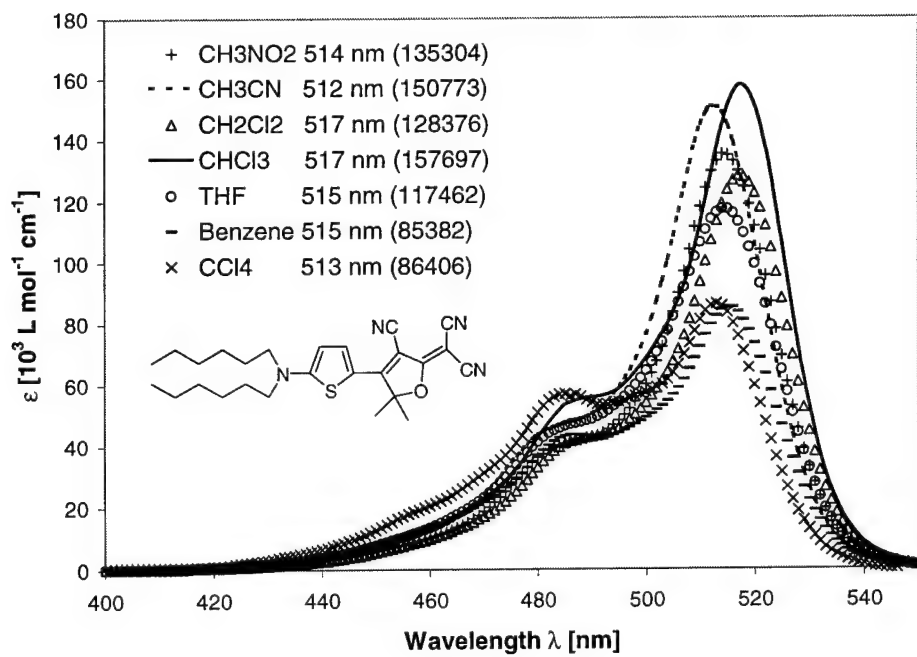
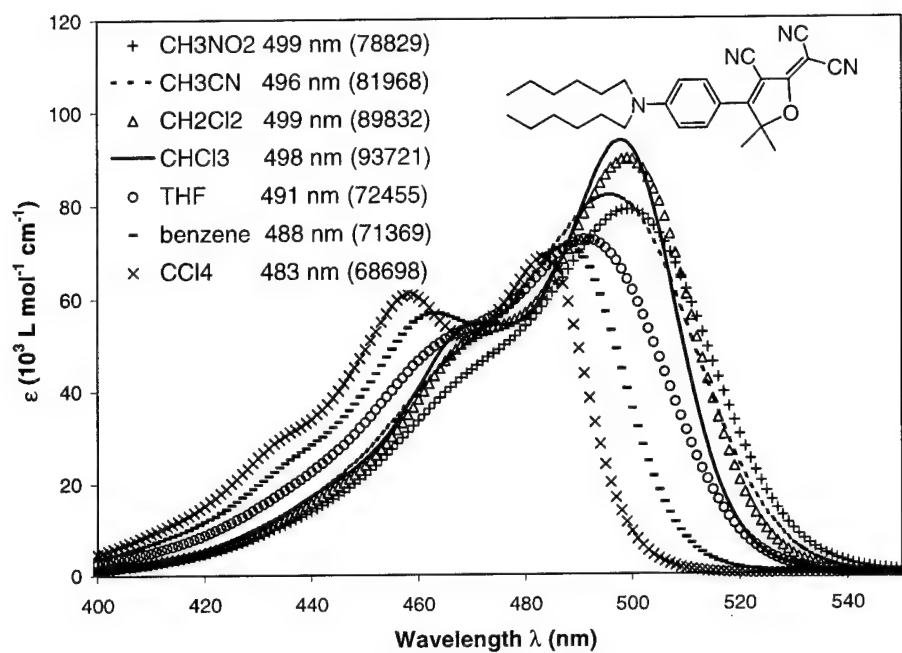


Figure 5. Top view and side view ORTEP drawings for crystalline DCDHF-C6M 52. The benzene containing pi-conjugated system is nearly planar. The donor is a cyclic amine and the dihydrofuran acceptor is substituted with a pair of methyl groups.

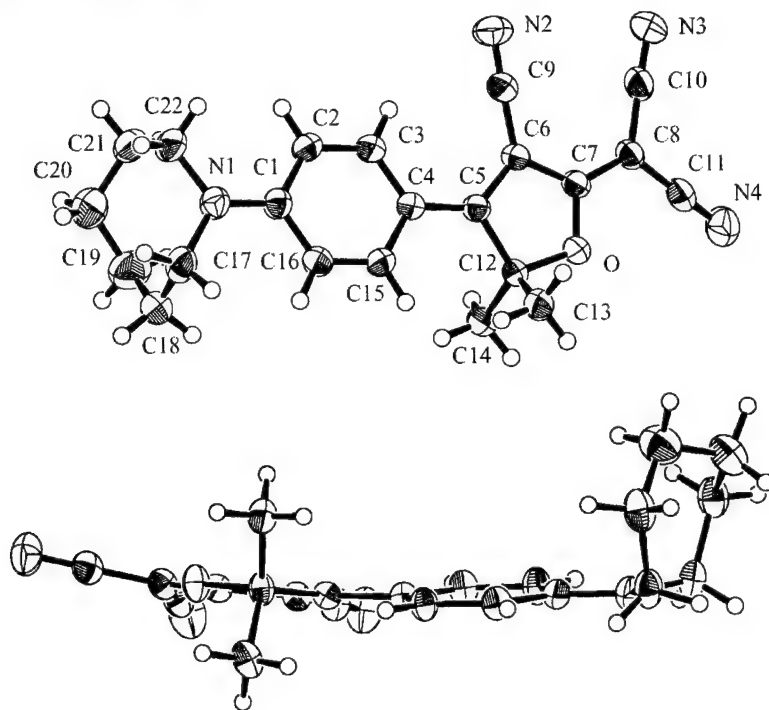
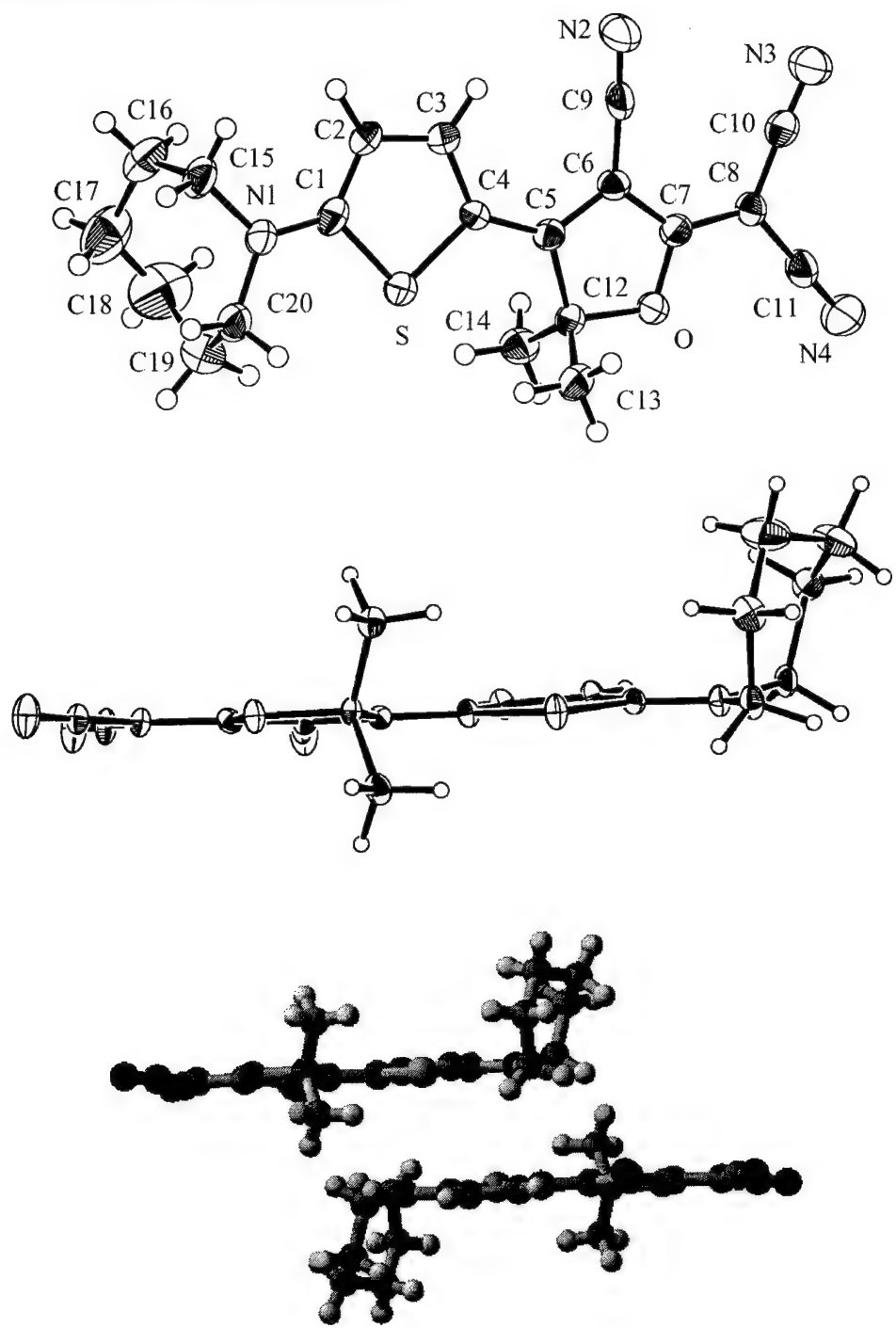


Table 1. Selected Bond Distances in Å for DCDHF-C6M in the crystal

atom 1	atom 2	L	atom 1	atom 2	L
C17	N1	1.467(3)	C7	C8	1.379(3)
C22	N1	1.464(3)	C8	C10	1.433(3)
N1	C1	1.357(2)	C10	N3	1.139(3)
C1	C2	1.411(3)	C8	C11	1.426(3)
C2	C3	1.366(3)	C11	N4	1.143(3)
C3	C4	1.410(3)	C5	C12	1.524(3)
C4	C5	1.432(3)	C7	O	1.331(2)
C5	C6	1.383(3)	C12	O	1.479(2)
C6	C9	1.427(3)	C4	C15	1.409(3)
C9	N2	1.142(2)	C15	C16	1.361(3)
C6	C7	1.436(3)	C1	C16	1.415(3)

Figure 6. Top view and side view ORTEP drawings for a single molecule and the packing diagram for thiophene core dimer TH-DCDHF-C6M 62 in the crystal. The donor is a cyclic amine and the dihydrofuran acceptor is substituted with a cycloaliphatic group.



5. Personnel Supported:

Postdoctoral researchers: Dr. Arosha Goonesekera (Stanford), Dr. Ueli Gubler (Stanford), Dr. Oksana Ostroverkhova (Stanford)

Graduate students: Dan Wright (Stanford, 1/2 salary support from AFOSR), Meng He (Kent), Yeonsuk Roh (no AFOSR salary support), Alexander Semyonov (Kent), Andre Leopold (Stanford, 2 months visitor from Univ. Bayreuth)

Visiting scientists: Prof. Ángela Sastre Santos (Kent, no AFOSR salary support)

Other: Shaumo Sadhukhan (part-time undergraduate)

6. Publications:

163. M. A. Díaz-García, D. Wright, J. D. Casperson, B. Smith, E. Glazer, W. E. Moerner, L. I. Sukhomlinova, and R. J. Twieg, "Photorefractive Properties of Poly(N-Vinyl Carbazole)-Based Composites for High Speed Applications," *Chem. Mater.* **11**, 1784-1791 (1999).
165. R. J. Twieg, M. He, L. Sukhomlinova, F. You, W. E. Moerner, M. A. Diaz-Garcia, D. Wright, J. D. Casperson, R. Wortmann, C. Glania, P. Kraemer, K. Lukaszuk, R. Matschiner, K. D. Singer, V. Ostoverkhov, and R. Petschek, "Design and Optimization of Chromophores for Liquid Crystal and Photorefractive Applications," *Proc. Mater. Res. Soc.* **561**, 119-130 (1999).
170. A. Goonesekera, D. Wright, and W. E. Moerner, "Image Amplification and Novelty Filtering in a Photorefractive Polymer," *Appl. Phys. Lett.* **76**, 3358-3360 (2000).
171. W. E. Moerner, "Photorefractive Polymers," in *Encyclopedia of Materials: Science and Technology*, Ed. D. D. Nolte; Senior Eds.: K.H. Jürgen Buschow, Robert W. Cahn, Merton C. Flemings, Bernhard Ilschner, Edward J. Kramer, Subhash Mahajan (Elsevier Science Ltd., Oxford, 2001) pp. 6961-6969.
174. M. A. Diaz-Garcia, D. Wright, J. D. Casperson, B. Smith, El Glazer, W. E. Moerner, L. I. Sukhomlinova, and R. J. Twieg, "High Speed PVK-Based Photorefractive Polymer Composites," *Nonlinear Optics* **25**, 189-194 (2000).
177. D. Wright, U. Gubler, M. B. Klein, and W. E. Moerner, "Photorefractive Polymers for Laser-Based Ultrasound Detection," *Proc. Soc. Photo-Opt. Instrum. Engr.* **4104**, 110-117 (2000).
179. M. He, R. J. Twieg, U. Gubler, D. Wright, and W. E. Moerner, "Synthesis and Properties of Some Composite Organic Photorefractive Materials," *Polym. Preprints* **42**, 510-511 (2001).
182. D. Wright, U. Gubler, S. Sadhukhan, W. E. Moerner, M. He, R. J. Twieg, M. DeClue, and J. Siegel, "Organic Photorefractive Material Design Strategies," *Proc. Soc. Photo-Opt. Instrum. Engr.* **4462**, 125-138 (2002).
184. U. Gubler, D. Wright, W. E. Moerner, and M. B. Klein, "Photochromic Polymers for the Optical Homodyne Detection of Ultrasonic Surface Displacements," *Opt. Lett.* **27**, 354-356

(2002).

185. D. Wright, U. Gubler, Y. Roh, W. E. Moerner, M. He, and R. J. Twieg, "A High Performance Photorefractive Polymer Composite with 2-dicyanomethylene-3-cyano-2,5-dihydrofuran Chromophore," *Appl. Phys. Lett.* **79**, 4274-4276 (2001).
186. U. Gubler, M. He, D. Wright, Y. Roh, R. J. Twieg, and W. E. Moerner, "Monolithic Photorefractive Organic Glasses with Large Coupling Gain and Strong Beam Fanning," *Adv. Mater.* **14**, 313-317 (2002).
188. O. Ostroverkhova, D. Wright, U. Gubler, W. E. Moerner, M. He, A. Sastre-Santos, R. J. Twieg, "Recent Advances in the Understanding and Development of Photorefractive Polymers and Glasses," *Adv. Func. Mater.* **12**, 621-629 (2002).
192. M. He, R. J. Twieg, U. Gubler, D. Wright, and W. E. Moerner, "Synthesis and Photorefractive Properties of Multifunctional Glasses," submitted to *Chem. Mater.* (2002).
193. M. He, R. Twieg, U. Gubler, D. Wright, and W. E. Moerner, "Synthesis and Properties of Glassy Organic Multifunctional Photorefractive Materials," appearing in *Opt. Mater.* (2002).
194. M. He, R. J. Twieg, O. Ostroverkhova, U. Gubler, D. Wright, W. E. Moerner, "Dicyanomethylenedihydrofuran photorefractive materials," *Proc. Soc. Photo-Opt. Instrum. Engr.* **4802**, 9-20 (2002).
195. O. Ostroverkhova, M. He, R. J. Twieg, W. E. Moerner, "High Performance Photorefractive Polymers and Glasses: Understanding Mechanisms and Limitations," *Proc. Soc. Photo-Opt. Instrum. Engr.* **4802**, 21-32 (2002).
197. K. Willets, O. Ostroverkhova, M. He, R. J. Twieg, and W. E. Moerner, "New Fluorophores for Single-Molecule Spectroscopy," *J. Amer. Chem. Soc.* (appearing 2003).
198. O. Ostroverkhova, W. E. Moerner, "High-Performance Photorefractive Organic Glass with Near-Infrared Sensitivity," submitted to *Appl. Phys. Lett.* (2002).
199. O. Ostroverkhova, M. He, R. J. Twieg, and W. E. Moerner, "Role of Temperature in Controlling Performance of Organic Photorefractive Glasses," submitted to *ChemPhysChem* (2002).

Taheri B, Munoz AF, Palffy-Muhoray P, Twieg R. Low threshold lasing in cholesteric liquid crystals MOL CRYST LIQ CRYST 358: 73-82 2001

Harris KD, Ayachitula R, Strutz SJ, Hayden LM, Twieg RJ Dual-use chromophores for photorefractive and irreversible photochromic applications APPL OPTICS 40: (17) 2895-2901 JUN 10 2001

Shiyanovskaya I, Singer KD, Twieg RJ, Sukhomlinova L, Gettwet V, "Electronic transport in smectic liquid crystals," *Phys. Rev. E* **65**, Art. No. 041715 (2002).

7. Interactions/Transitions:

(a) Invited participations/presentations at meetings, conferences, seminars, etc.

169. W. E. Moerner, D. Wright, A. Goonesekera, M. A. Diaz-Garcia, and R. J. Twieg, "Trap Dynamics in Photorefractive Polymer Composites," Materials Research Society Fall Meeting, Boston, Massachusetts, November 29 - December 3, 1999.
194. W. E. Moerner, "Mechanisms of Photorefractivity in Polymer Composites," Northwestern University Organic Materials Symposium, Evanston, Illinois, November 17, 2000.
195. W. E. Moerner, D. Wright, A. Goonesekera, M. DeClue, J. S. Siegel, and R. J. Twieg, "Trap Dynamics in Photorefractive Polymers: Mechanisms and Applications," Symposium on Field-Responsive Polymers, American Chemical Society POLY Millenial 2000, Waikoloa, Hawaii, December 9-13, 2000.
196. W. E. Moerner, D. Wright, U. Gubler, A. Goonesekera, M. DeClue, J. S. Siegel, M. He, and R. J. Twieg, "Recent Progress in Photorefractive Polymers: Mechanisms and Applications," International Congress of Pacific Basin Societies, Pacificchem 2000, Honolulu, Oahu, Hawaii, December 14-19, 2000.
206. W. E. Moerner, "Photorefractive Polymers: What They Are and What You Can Do With Them," Quantum Electronics Seminar, Department of Applied Physics, Stanford University, Stanford, California, April 16, 2001.
207. D. Wright, U. Gubler, W. E. Moerner, M. He, R. J. Twieg, M. DeClue, and J. S. Siegel, "Photorefractive Polymer Design Strategies," Society of Photo-Optical Instrumentation Engineers Annual Meeting, San Diego, California, July 29 - August 3, 2001.
212. W. E. Moerner, D. Wright, U. Gubler, O. Ostroverkhova, M. He, A. Sastre-Santos, and R. J. Twieg, "Recent Advances in the Understanding and Development of Photorefractive Polymers and Glasses," Sixth International Conference on Organic Nonlinear Optics, ICONO'6, Tucson, Arizona, December 16-20, 2001.
215. O. Ostroverkhova, U. Gubler, D. Wright, M. He, R. J. Twieg, and W. E. Moerner, "High-Performance Photorefractive Organic Glasses: Understanding Mechanisms and Limitations," Society of Photo-Optical Instrumentation Engineers Annual Meeting, Seattle, Washington, July 7-11, 2002.

(b) Other presentations at meetings, conferences, seminars, etc.

U. Gubler and W. E. Moerner, "Mechanisms of Photorefractivity in Polymeric Materials," AFOSR PR Polymer Review, San Diego, CA, July 28, 2001.

D. Wright, U. Gubler, W. E. Moerner, M. DeClue, and J. Siegel, "A New Charge Transport Polymer for Photorefractive Applications," Conference on Lasers and Electro-Optics, CLEO 2001, Baltimore, Maryland, May 6-11, 2001.

U. Gubler, D. Wright, W. E. Moerner, and M. B. Klein, "Photorefractive and Photochromic Polymers as Adaptive Beam Combiners for Laser-Based Ultrasound Detection," Conference on Lasers and Electro-Optics, CLEO 2001, Baltimore, Maryland, May 6-11, 2001.

(c) Interactions, transitions with Air Force organizations:

- (a) W. E. Moerner, Stanford University, with chromophores from R. J. Twieg, Kent State
- (b) Photorefractive polymer samples,
- (c) Dr. Marvin Klein, Lasson Technologies, 310-216-4046,
- (d) for detection of laser-based ultrasonic waves for nondestructive evaluation

Samples provided to Dr. Fassil Gebremichael have now been studied at the Air Force Academy. Samples even three years old showed useful photorefractive effects, as reported by Dr. Gebremichael at the 2001 PR Polymer Review meeting.

A new set of samples with the composition PVK:AODCST:BBP:TNF were provided to Dr. Fassil Gebremichael on July 12, 2001, along with experimental measurements of gain coefficient at 830 nm. These samples will be used for optical experiments in the infrared.

Several detailed analyses of PR polymers for opposite geometry limiting in fibers have been provided to Dr. Mark Kuzyk, most notably a detailed report on 8 February 2001.

A sample of PMMA-DR1 (10 mer% DR1) were provided to Dr. Mark Kuzyk on August 20, 2001, for use in fabricating cores of optical fibers for laser protection.

A sample of TZT, a saturable absorber molecule, were provided to Dr. Mark Kuzyk on August 20, 2001, for possible use in low power limiting applications at 514 or 532 nm.

Table of All DCDHF Chromophores prepared in AFOSR Study (page 1 of 2)

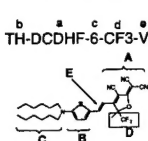
$\lambda_{\text{max}}(\text{HF})$ (ϵ_{max} (L cm^{-1} mol^{-1}))	Mp (DSC) ($^{\circ}\text{C}$)	^1Tg ($^{\circ}\text{C}$)	$^1\text{Tg}_{\text{rec}}$ ($^{\circ}\text{C}$)	^1Td (TGA) ($^{\circ}\text{C}$)	HOM O (eV) ²	Compd	Chemical Structure	MW (g mol ⁻¹)	λ_{max} (nm) dioxane	ϵ_{max} (L cm^{-1} mol ⁻¹)	μ_{eff} (10^{-30} C m)	μ_2 (10^{-30} C m)	$\Delta\mu$ (10^{-30} C m)	c^2	$\Delta\mu_{\text{ext}}$ (10^{-30} C m ⁻¹ m ³)	β_0 (10^{-30} C V ⁻² m ³)	β_0^{local} (10^{-74} C ² V ⁻² m ³ kg ⁻¹ mol)	F_0^{ext} (10^{-74} C ² V ⁻² m ³ kg ⁻¹ mol)		
486 (68600)	183	36 ^a	71 ^a 89 ^a	312	-5.63	Mb04075 DCDHF-MOE		392.45	477	55000	29	37	31	0.26	66	40	90	0.85	0.76	
483	>278	no	no	278 (at mp)		Insol	Mb04052 DCDHF-1		304.35											
491 (74300)	249	16 ^a	122 ^a 134 ^a	299			Mb04102 DCDHF-C6M		358.44	482	62000	29	39	33	0.25	67	41	98	1.07	0.94
491 (62600)	305	no	no	319			Mb04104 DCDHF-C5MDM		372.46											
488 (64400)	250	69	107 131	292			TJ01001 (Mb04117) DCDHF-2		332.4	480	67000	30	38	28	0.29	66	43	88	1.01	1.01
490 (76600)	278	no	no	313			TJ01003 DCDHF-3		360.45											
491 (72600)	250	no	no	311	-5.59		Mb04147 DCDHF-4		388.51											
491 (77000)	169	no	no	312			Mb04111 DCDHF-5		416.56											
491 (72500)	129	19 ^a	75 ^a 91 ^a	320	-5.56		Mb04070 DCDHF-6		444.61	483	70200	31	38	28	0.29	68	47	95	0.82	0.81
492 (76700)	123	1 ^a	66 ^a 78 ^a	322			Mb04103 DCDHF-8		500.72											
492 (70500)	171	12	58 64	313	-5.57		Mb04100 DCDHF-2EH		500.72											
492 (74700)	150	33	84 99	318	-5.54		Mb04096 DCDHF-6-C7M		512.73	484	68900	30	36	27	0.29	66	44	87	0.61	0.59
493 (74300)	95	2 ^a	Stable ^a	326			Mb04114 DCDHF-6-DB		528.77											
520 (75400)	214	76 ^a	stable ^a	275			Mb05041 DCDHF-C6M-CF ₃		412.41											
520 (75800)	130	17 ^a	Stable ^a	310	-5.61		Mb04141 DCDHF-6-CF ₃		498.58	509	73000	31	40	34	0.26	71	49	129	1.03	0.86
517 (75800)	180	64 ^a	Stable ^a	277			Mb05012 DCDHF-2-CF ₃		386.37	505	75500	32	38	35	0.26	73	52	139	1.37	1.07
515 (117500)	134	22 ^a	98 ^a 113 ^a	308	-5.47		Mb05008 TH-DCDHF-6		450.64	512	108000	31	46	11	0.41	63	50	42	0.43	1.17
513 (118000)	264	89 ^a	146 ^a 170 ^a	332	-5.46		Mb04137 TH-DCDHF-C6M		364.47	510	109000	30	47	11	0.41	61	46	39	0.50	1.41
620 (172000)	172	no	no	298	-5.16		Mb05046 TH-DCDHF-6-V		476.68	610	109600	37	48	15	0.40	76	84	116	1.17	2.08
570 (70200)	245	no	no	246 (at mp)	-5.32		Mb04044 DCDHF-2-V		358.44	542	60500	35	39	44	0.23	83	67	241	2.62	1.51
606 (69100)	243	no	no	239 (at mp)			Mb05014 DCDHF-J-V		382.46	582	66000	34	46	49	0.21	84	68	292	3.51	2.14
577 (76500)	140K 147	34	107	262			Mb05111 DCDHF-6-V		470.65											
574 (50900)	100	22	Stable	309	-5.32		As01025 DCDHF-2EH-V		526.76	556	56600	33	42	52	0.19	84	61	266	2.12	1.18
							TJ0100 ^a DCDHF-CSM-V													
561 (65500)	212	no	no	278	-5.34		Mb03136 DCDHF-MOE-V		418.49	530	58900	34	40	54	0.19	87	62	267	2.55	1.38
537 (50000)	331	no	no	336 (at mp)	-5.45		Mb04076 DCDHF-DPH-V		454.52	538	51000	34	28	61	0.17	91	63	310	1.91	0.70
572 (67200)	glass	141	Stable glass	270			Mb05058 DCTA-6C-DCDHF-V		1004.2	539	60300	35	40	53	0.20	88	66	287	1.14	0.62

Table of All DCDHF Chromophores prepared in AFOSR Study (page 2 of 2)

511 (99000)	237.4	76	112 118	320	-5.24 Irrever sible onset value	Mh05087 2EHO-D-DCDHF		508.65												
511 (98000)	181	69	Stable glass	324	-5.23 Irrever sible onset value	Mh05100 M2EHO-DDCDHF		508.65												
606 (66200)	No mp	no	no	239		Mh05107 DCDHF-2-2V														
540 (83000)	<i>Glazt1</i> <i>57crys</i> <i>tal184J</i>	103	154 168	309	-5.32 Irrever sible onset value	Mh05064 PFP-DDCDHF		670.42	545	72750	30	36	-10	0.58	61	49	-41	-0.22	0.44	
531 (87600)	193	57	Stable glass	318	-5.28 Irrever sible onset value	Mh05060 HP-DDCDHF		436.55	538	84100	31	49	-9	0.57	63	52	-38	-0.43	1.35	
540 (85800)	glass	64	Stable glass	314	-5.29 Irrever sible onset value	Mh05065 DOCP-DDCDHF		564.72	547	77350	31	43	-8	0.56	63	53	-35	-0.27	0.82	
	290	no	no	310		Mh05078 P-DDCDHF		380.44												

1 Tg (glass transition temperature) and Trec (recrystallization temperature) are measured by cooling melted samples (cooling rate 10 °C/min. A rate of 30 °C/min for the numbers with * and 5 °C/min for the numbers with *) followed by second heating with 10 °C/min. Two recrystallization temperatures were recorded: first number is the onset value of the recrystallization and second number is the peak value. TGA is measured by heating the sample from rt to 1000 °C. Td is the decomposition temperature determined from both TGA and DSC.

2 HOMO is calculated from CV measurement. Conditions for CV: Pt electrode, Pt disk and Hg/HgCl₂/NaCl reference electrode, 0.1 M tetraethylammonium tetrafluoroborate in acetonitrile as supporting electrolyte, speed: 300 mV/sec.



- DCDHF is the core part of the name, which refers to part A.
- If part B is a thiophene, then TH is put to the left of DCDHF. If part B is a phenyl, then nothing to the left of DCDHF.
- The numbers or letters next to DCDHF represent the substitutions on nitrogen (part C). (numbers mean the number of alkyl carbons: MOE: methoxyethyl; C6M: cyclic 6 methylene; C5MDM: cyclic 5 methylenes with two methyls; 2EH: 2-ethylhexyl; J: julolidine; DPH: diphenyl).
- If there are substitutions other than two methyls on part D, they are represented after step c. (DB: dibutyl; CF3: trifluoromethyl; C6M: cyclic 6 methylenes).
- If there is a vinyl link in the molecule (part E), then at the end of the name, a V is used.